UCLA
COMPUTATIONAL AND APPLIED MATHEMATICS

Pole Dynamics and Oscillations for Complex Burgers Equation in the Small Dispersion Limit

David Senouf
Russel Caflisch
Nicholas Ercolani

August 1995

CAM Report 95-38

Department of Mathematics
University of California, Los Angeles
Los Angeles, CA. 90024-1555

POLE DYNAMICS AND OSCILLATIONS FOR COMPLEX BURGERS EQUATION IN THE SMALL DISPERSION LIMIT

D. SENOUF[†,¶] R. CAFLISCH[‡,¶] AND N. ERCOLANI[§,**]

Abstract. A meromorphic solution to Burgers' equation with complex viscosity is analyzed. The equation is linearized via the Cole-Hopf transform which allows for a careful study of the behavior of the singularities of the solution. The asymptotic behavior of the solution as the dispersion coefficient tends to zero is derived. For small dispersion, the time evolution of the poles is found by numerically solving a truncated infinite dimensional Calogero type dynamical system. This system represents a set of compatibility conditions derived from the PDE and a Mittag-Leffler (pole) expansion of the solution. The initial data is provided by high order asymptotic approximations of the poles at the critical time t_* for the dispersionless solution via the method of steepest descents. The solution is re-constructed using the pole expansion and the location of the poles. The oscillations observed via the singularities are compared to those obtained by a classical stationary phase analysis of the solution as the dispersion parameter $\epsilon \to 0^+$. A uniform asymptotic expansion as $\epsilon \to 0^+$ of the dispersive solution is derived in terms of the Pearcey integral in a neighborhood of the caustic. A continuum limit of the pole expansion and the Calogero system is obtained, yielding a new integral representation of the solution to the inviscid Burgers' equation.

AMS subject classifications. 35A20, 35A40, 35B40, 35Q53, 41A60

1. Introduction. Many nonlinear dispersive systems exhibit rapid oscillations in their spatial-temporal dependence in the regime of small dispersion. Examples include PDEs such as the Korteweg-de Vries (KdV) equation, the nonlinear Schrödinger equation [16, 17, 24], and finite difference equations such as the Lax-Wendroff method (see also [25]). Although a fascinating mathematical phenomena, these oscillations are generally quite difficult to describe and control and are an obstacle to the efficiency of numerical and analytical methods. A complete analysis of oscillations would include a slowly-varying description of their shape, amplitude, wavelength and phase. However, these features have been successfully analyzed only for a few completely integrable systems such as the KdV equation.

Burgers equation with an imaginary "viscosity" coefficient $\nu = i\epsilon$, given by

$$\psi_t + \psi\psi_x = i\epsilon\psi_{xx}, \quad \epsilon \geqslant 0 \tag{1.1}$$

was first described by Dobrokhotov *et altri* in [15]. It is perhaps the simplest example of a non linear dispersive equation, but has received surprisingly little attention. This equation has the same linear part $(\psi_t - i\epsilon\psi_{xx})$ as the Schrödinger equation, and as such can be referred to as the Schrödinger equation with convective nonlinearity. We do not know of any applications in which this equation arises, and it does not seem to have a Hamiltonian structure. Moreover, the system is nonlinearly ill-posed at least for

[†] To whom correspondence should be sent: 4 rue Jean Ferrandi, Paris 75006, FRANCE.

[‡] Department of Mathematics, UCLA, Los Angeles, California 90095-1555. (caflisch@math.ucla.edu).

[§] Department of Mathematics, University of Arizona, Tucson, Arizona 85721. (ercolani@math.arizona.edu).

[¶] Research partially supported by NSF Grant # DMS-9306720.

[**] Research partially supported by Grant # 0000000.

certain complex values of ν, since singularities can occur in finite time. Nevertheless, we believe that this equation is an interesting mathematical prototype for dispersive (imaginary ν) or mixed dissipative-dispersive systems (complex ν).

In this paper, we present a numerical and analytic study of solutions to (1.1) for complex values of ν. The solution to equation (1.1) can be solved using the Cole-Hopf non linear transform which yields an integral representation involving the heat kernel. For small $|\nu| = \epsilon$, the resulting formula for ψ_ν can be approximated using the *stationary phase* method. A new method used to compute the solution is found through *pole dynamics.* This method is based on obtaining the time dependent locations of the complex poles of the function ψ_ν by solving an infinite system of coupled ODEs. The solution ψ_ν is then found by computing its Mittag-Leffler expansion which involves the position of the poles. One can also compute ψ_ν directly through a *finite difference method,* at least for times before a pole hits the real axis. Finally, in the zero-dispersion (or zero-viscosity limit) $\nu \to 0$, the poles coalesce onto a branch-cut, and the zero-dispersion solution is described by *branch-cut dynamics.* This method may be of general interest as a new (to the best of our knowledge) method for solving the inviscid Burgers equation.

These methods will be formulated in general, but they will be numerically evaluated for a special choice of initial data, namely the cubic polynomial

$$\psi(x,0) = 4x^3 - x/t_* \tag{1.2}$$

which is chosen for its generic features for the inviscid equation (see [3, 18, 28]). In this initial data, t_* is positive and corresponds to the time of first singularity formation for the inviscid problem. The cube root singularity found at the origin at $t = t_*$ is known to be a generic singularity for the inviscid Burgers equation. It is due to the coalescence of two conjugate branch points of order two in the complex plane. For further details, see [3, 4, 8, 18]. Moreover both cases $\nu = 0$ and $\nu \neq 0$ can be completely analyzed, and in the case $\nu \neq 0$, there is an instantaneous generation at $t > 0$ of a countable set of complex spatial simple poles. For this initial data, the small dispersion ($\epsilon \to 0^+$) stationary phase approximation of the solution and its zeroes can be evaluated rather explicitly, at least for $t = t_*$.

There are three main points to this work: First, in the purely dispersive case in which ν is imaginary and small, the solution ψ_ν of (1.1) develops rapid oscillations. Second, these oscillations are caused by the presence of complex poles in ψ which have moved close to the real axis. This result, which is clearly demonstrated below through comparison of the pole dynamics with the solution on the real axis, is important in providing a tangible cause for the formation of the oscillations. Third, the branch cut dynamics provide a slowly varying but incomplete description of the pole locations. Although, we have not yet succeeded in deriving a slowly varying description of the oscillations themselves, we believe that the branch cut dynamics represents a promising start.

In order to investigate the positions of the poles, we derive a Calogero-type infinite dimensional dynamical system by replacing the pole-expansion of the solution into the PDE. We then solve numerically a truncated version of this system, where the initial data is generated by asymptotic and numerical approximations of the poles at the inviscid pre-shock time t_*. The numerical resolution of the stationary solution of Calogero dynamical system has previously been used in [32] to obtain the stationary positions of the poles of the solution to a flame front equation. In the case $\nu > 0$, the

poles are fixed to the imaginary axis and move towards the origin until $t \approx t_*$, after which they turn around and move away as t increases (see [29]). When dispersion is added, i.e. $\theta = \arg\nu \neq 0$, the poles are no longer confined to the imaginary axis and evolve in the complex plane describing intricate motions. When $\nu = i\epsilon$ ($\epsilon > 0$) is a purely dispersive coefficient, the poles spiral around the real axis. The proximity of the poles to the real axis generates oscillations which are observed by reconstructing the solution numerically via the pole expansion and the pole dynamics.

2. Integral representation, pole expansion and pole dynamics for $\nu > 0$. We recall some results that are derived in [29]. In this case we let $\psi_\nu = u_\nu$ to be consistent with the familiar notation that is used in the classical Burgers equation. For $\nu > 0$, the Cole-Hopf transform $u_\nu = -2\nu\,\partial_x \log(\phi_\nu)$ linearizes equation (3.1) into the diffusion equation for ϕ_ν. Thus the solution is given by

$$u_\nu(x,t) = \frac{x}{t} - 2\nu\,\partial_x \log\big(E_\nu(x,t)\big) = \frac{x}{t} - \frac{U_\nu(x,t)}{t}, \tag{2.1a}$$

$$E_\nu(x,t) = \int_{-\infty}^{\infty} \exp\left\{\frac{1}{2\nu}\left(\frac{x}{t}y + \alpha y^2 - y^4\right)\right\} dy, \tag{2.1b}$$

where $\alpha = \frac{t-t_*}{2it_*} \in \mathbb{R}$. The function $E_\nu(x,t)$ has the following properties for fixed $t, \nu > 0$:

- It is an even entire function of x.
- Its order $\lambda = 4/3$.
- Its genus $h = 1$.
- It has infinitely many conjugate and opposite zeros on the imaginary axis.
- The order of convergence of the zeros is the order $\lambda = 4/3$, i.e. $\sum_n 1/|a_n|^{\lambda+\varepsilon} < +\infty$, $\forall \varepsilon > 0$.

The fact that the zeros are imaginary is proved by Pólya in [27]. Combining these properties, $E_\nu(x,t)$ has an infinite product representation in terms of its zeros which we denote by $x = \pm a_n = \pm i\beta_n$:

$$E_\nu(x,t) = \mathcal{C}_\nu(t) \prod_{n=1}^{\infty} \left(1 + \frac{x^2}{\beta_n^2(t,\nu)}\right), \quad \sum_n \frac{1}{\beta_n} = +\infty, \quad \sum_n \frac{1}{\beta_n^2} < +\infty, \tag{2.2a}$$

$$\mathcal{C}_\nu(t) = E_\nu(0,t) = \int_{-\infty}^{+\infty} e^{\frac{1}{2\nu}(\alpha y^2 - y^4)}\, dy = \frac{\sqrt{\alpha}}{2}\, e^{\frac{\alpha^2}{16\nu}}\, K_{1/4}\left(\frac{\alpha^2}{16\nu}\right), \tag{2.2b}$$

where $\mathcal{C}_\nu(t_*) = \nu^{1/4} 2^{-3/4}\Gamma(1/4)$, $K_q(z)$ is the modified Bessel function of the second kind, and $K_{1/4}(z) = \mathcal{O}(z^{-1/4})$ as $z \to 0$. After logarithmic differentiation of E_ν, using (2.1a) and (2.2a), the singular part of the solution being the ratio of two entire functions with zeros is meromorphic. Thus we find an infinite pole expansion of Mittag-Leffler type for the solution which converges uniformly on compact sets for x away from the poles $x = \pm i\beta_n$:

$$u_\nu(x,t) = \frac{x}{t} - \frac{U_\nu(x,t)}{t} = \frac{x}{t} - \sum_{n=1}^{\infty} \frac{4\nu x}{x^2 + \beta_n^2(t,\nu)}, \tag{2.3}$$

where $U_\nu(x,t)$ is the spatially singular part of the viscous solution defined by

$$U_\nu(x,t) = x - t\,u_\nu(x,t) = t \cdot \sum_{n=1}^{\infty} \frac{4\nu x}{x^2 + \beta_n^2(t,\nu)}. \tag{2.4}$$

Note that u_ν can be expressed in a more symmetric way as

$$u_\nu(x,t) = \frac{x}{t} - 2\nu \sum_{\substack{n=-\infty \\ n\neq 0}}^{\infty} \frac{1}{x - i\beta_n(t,\nu)}, \tag{2.5}$$

where we use the convention that $\beta_{-n} = -\beta_n$. Let

$$\forall n \in \mathbb{N}^* = \mathbb{N}\backslash\{0\}, \quad \dot{\beta}_n = \frac{d\beta_n}{dt}, \tag{2.6}$$

then we replace the full Mittag-Leffler/pole expansion found in (2.3) in the PDE $u_t + u\,u_x = \nu\,u_{xx}$. Using partial fraction expansions, we find (see [29] for more details)

$$\dot{\beta}_n = \frac{\beta_n}{t} + \frac{\nu}{\beta_n} - 4\nu\beta_n \sum_{\substack{l=1 \\ l\neq n}}^{\infty} \frac{1}{\beta_l^2 - \beta_n^2}. \tag{2.7}$$

Similarly to (2.5), there is a more symmetric formulation to the dynamical system (2.7) given by

$$\dot{\beta}_n = \frac{\beta_n}{t} - 2\nu \sum_{\substack{l=-\infty \\ l\neq n,0}}^{\infty} \frac{1}{\beta_l - \beta_n}. \tag{2.8}$$

Note that the pole expansion (2.5) and the dynamical system (2.8) represent a general solution to Burgers' equation which is independent of the initial data.

Multiplying (2.7) by β_n and introducing the variable

$$\gamma_n(t,\nu) = \frac{\beta_n^2(t,\nu)}{\nu}, \tag{2.9}$$

we have $\sum_n \gamma_n^{-1} < +\infty$, and system (2.7) becomes independent of ν:

$$\forall n \in \mathbb{N}^*, \quad \frac{\dot{\gamma}_n}{2} = \frac{\gamma_n}{t} + 1 - 4\gamma_n \sum_{\substack{l=1 \\ l\neq n}}^{\infty} \frac{1}{\gamma_l - \gamma_n}. \tag{2.10}$$

3. Integral representation, pole expansion and pole dynamics for $\nu \in \mathbb{C}^+$. In the analysis that follows, we take advantage of the complete integrability of Burgers' model of a one-dimensional fluid, and allow for the viscosity coefficient ν to take complex values of the form $\nu = \epsilon e^{i\theta}$, $\epsilon > 0$ and $|\theta| \leq \pi/2$. Then $\psi = \psi_\nu(x,t)$ satisfies

$$\frac{\partial\psi}{\partial t} + \psi\,\frac{\partial\psi}{\partial x} = \nu\,\frac{\partial^2\psi}{\partial x^2}, \qquad x \in \mathbb{R}, t > 0, \nu \in \mathbb{C}^+, \tag{3.1}$$

where

$$\mathbb{C}^+ \equiv \{\nu \in \mathbb{C} \text{ s.t. } |\nu| > 0 \text{ and } |\arg\nu| \leqslant \pi/2\} = \{\nu \mid \Re\nu \geqslant 0, \nu \neq 0\}. \tag{3.2}$$

We can express this complex PDE as a system of 2 real coupled PDEs: Let $\psi = \psi_R + i\psi_I$ where $\psi_R = \Re\psi$ and $\psi_I = \Im\psi$, then (3.1) becomes

$$\partial_t \begin{pmatrix} \psi_R \\ \psi_I \end{pmatrix} + \begin{pmatrix} \psi_R & -\psi_I \\ \psi_I & \psi_R \end{pmatrix} \partial_x \begin{pmatrix} \psi_R \\ \psi_I \end{pmatrix} = \epsilon \begin{pmatrix} \cos\theta & -\sin\theta \\ \sin\theta & \cos\theta \end{pmatrix} \partial_{xx} \begin{pmatrix} \psi_R \\ \psi_I \end{pmatrix}. \tag{3.3}$$

When this coefficient is purely imaginary, $\nu = i\epsilon$, $\epsilon > 0$, (3.3) can be thought of as the nonlinear Schrödinger equation with convective nonlinearity:

$$\frac{\partial \psi}{\partial t} + \psi \frac{\partial \psi}{\partial x} = i\epsilon \frac{\partial^2 \psi}{\partial x^2}, \qquad x \in \mathbb{C}, t > 0, \epsilon \geqslant 0. \tag{3.4}$$

From the integral definition of $E_\nu(x,t)$ in (2.1b), one can extend the ν-domain of validity to complex values of ν: Let $\nu = \epsilon e^{i\theta} \in \mathbb{C}^+$, then

$$E_\nu(x,t) = E_{\epsilon e^{i\theta}}(x,t) = \int_{-\infty}^{\infty} \exp\left\{ \frac{e^{-i\theta}}{2\epsilon} \left(\frac{x}{t} y + \alpha y^2 - y^4 \right) \right\} dy. \tag{3.5}$$

It is straightforward that in order for the integral (3.5) to remain convergent, we must have $\Re\nu \geqslant 0$, i.e. $|\theta| \leqslant \pi/2$. This can be verified by using Jordan's lemma and deforming the contour of integration along the ray $\arg y = \theta/4$ for $0 \leqslant \theta \leqslant \pi/2$ so that $E_\nu(x,t)$ can be written as

$$E_\nu(x,t) = e^{i\theta/4} \int_{-\infty}^{\infty} \exp\left\{ \frac{1}{2\epsilon} \left(\frac{x}{t} y e^{-i\frac{3\theta}{4}} + \alpha e^{-i\frac{\theta}{2}} y^2 - y^4 \right) \right\} dy. \tag{3.6}$$

Thus in the range $0 \leqslant \theta \leqslant \pi/2$, the function $E_\nu(x,t)$ is again an entire function of x of order $\lambda = 4/3$, and as such it also has infinitely many zeros [5]. Noticing the symmetry relation

$$E_{\overline{\nu}}(x,t) = \overline{E_\nu(\overline{x},t)}, \tag{3.7}$$

we can extend the domain of validity of representation (3.6) to the range $|\theta| \leqslant \pi/2$. The even parity of $E_\nu(x,t)$ as a function of x is preserved so that

$$E_\nu(-x,t) = E_\nu(x,t). \tag{3.8}$$

The zeros of $E_\nu(x,t)$ therefore come in opposite pairs $x_n = \pm a_n(t,\nu)$, with the property that for each fixed $t > 0$ and fixed $\nu \in \mathbb{C}^+$,

$$\sum_n \frac{1}{|a_n|} = +\infty, \quad \sum_n \frac{1}{|a_n|^2} < +\infty.$$

The infinite product representation of E_ν is now

$$E_\nu(x,t) = C_\nu(t) \prod_{n=1}^{\infty} \left(1 - \frac{x^2}{a_n^2(t,\nu)} \right), \tag{3.9}$$

so that the Mittag-Leffler/pole expansion becomes

$$\psi_\nu(x,t) = \frac{x}{t} - \frac{\Psi_\nu(x,t)}{t} = \frac{x}{t} - \sum_{n=1}^{\infty} \frac{4\nu x}{x^2 - a_n^2(t,\nu)}, \tag{3.10}$$

where the spatially singular part of the pole expansion is given by

$$\Psi_\nu(x,t) = x - t\,\psi_\nu(x,t) = t \cdot \sum_{n=1}^{\infty} \frac{4\nu x}{x^2 - a_n^2(t,\nu)}. \tag{3.11}$$

As in (2.5), ψ_ν can be expressed in a more symmetric way as

$$\psi_\nu(x,t) = \frac{x}{t} - 2\nu \sum_{\substack{n=-\infty \\ n\neq 0}}^{\infty} \frac{1}{x - a_n(t,\nu)}. \tag{3.12}$$

Letting $\beta_n = -ia_n$ in (2.7), one finds the associated Calogero dynamical system for arbitrary $\nu \in \mathbb{C}^+$: Let

$$\dot{a}_n = \frac{da_n}{dt}, \quad a_{-n} = -a_n,$$

then

$$\dot{a}_n = \frac{a_n}{t} - \frac{\nu}{a_n} - 4\nu a_n \sum_{\substack{l=1 \\ l\neq n}}^{\infty} \frac{1}{a_n^2 - a_l^2}, \qquad \forall n \in \mathbb{N}^*. \tag{3.13}$$

As in (2.8), one can express (3.13) in a more symmetric way as

$$\dot{a}_n = \frac{a_n}{t} - 2\nu \sum_{\substack{l=-\infty \\ l\neq n,0}}^{\infty} \frac{1}{a_n - a_l}, \qquad \forall n \in \mathbb{N}^*. \tag{3.14}$$

Note finally that the pole expansion (3.12) and the dynamical system (3.14) represent a general solution to Burgers' equation which is independent of the initial data.

One can further simplify (3.13) by multiplying both sides by a_n and introducing the variable

$$\kappa_n = \frac{a_n^2}{\nu}. \tag{3.15}$$

The corresponding system of ordinary differential equations (3.13) becomes free of ν so that

$$\frac{1}{2}\frac{d\kappa_n}{dt} = \frac{\dot{\kappa}_n}{2} = \frac{\kappa_n}{t} - 1 - 4\kappa_n \sum_{\substack{l=1 \\ l\neq n}}^{\infty} \frac{1}{\kappa_n - \kappa_l}, \quad \forall n \in \mathbb{N}^*. \tag{3.16}$$

4. Exact pole locations at t_* for $\nu \in \mathbb{C}^+$. At $t = t_*$, since $\alpha = 0$, we have for $|x| < \infty$

$$E_\nu(x,t_*) = e^{i\theta/4} \int_{-\infty}^{\infty} \exp\left\{\frac{1}{2\epsilon}\left(\frac{x}{t_*}e^{-i3\theta/4}y - y^4\right)\right\} dy. \tag{4.1}$$

Thus using Pólya's theorem once more (cf. [27]), the zeros of $E_\nu(x,t_*)$ denoted by $\pm a_n(t_*,\nu)$ are located on the ray $\arg x = 3\theta/4 + \pi/2$, with absolute value $|a_n(t_*,\nu)| = \beta_n(t_*,\epsilon) > 0$, where $\pm i\beta_n(t_*,\epsilon)$ is the n-th ordered zero of $E_\epsilon(x,t_*)$ on the imaginary axis. For $\nu = \epsilon e^{i\theta} \in \mathbb{C}^+$, the zeros of $E_\nu(x,t)$ are thus located at the complex positions

$$x = \pm a_n(t_*, \nu = \epsilon e^{i\theta}) = \pm e^{i3\theta/4}\, i\beta_n(t_*,\epsilon), \qquad \forall n \in \mathbb{N}^*. \tag{4.2}$$

See Fig. 4.1 for the positions of the poles at $t = t_*$. Thus, in order to describe the

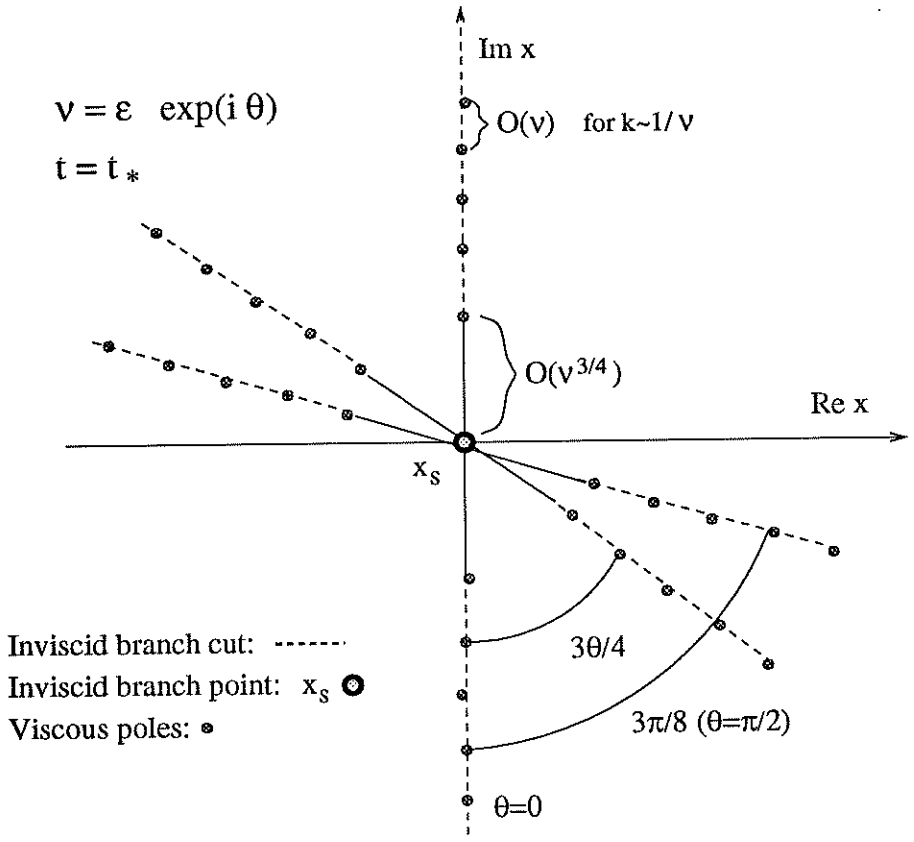

FIG. 4.1. *Inviscid branch point, branch cuts and viscous poles at $t = t_*$ for $\nu = |\nu|e^{i\theta}$ $(|\theta| \le \pi/2)$*

asymptotic behavior of the zeros of $E_\nu(x, t_*)$, we place ourselves on the ray $\arg x = 3\theta/4 + \pi/2$, so that at the pre-shock time t_*, letting $\nu = \epsilon e^{i\theta}$,

$$\begin{aligned} E_{\epsilon e^{i\theta}}(e^{i3\theta/4} i\beta, t_*) &= e^{i\theta/4} \int_{-\infty}^{\infty} \exp\left\{\frac{1}{2\epsilon}\left(\frac{i\beta}{t_*} y - y^4\right)\right\} dy \\ &= e^{i\theta/4} E_\epsilon(i\beta, t_*) \\ &= e^{i\theta/4} \left(\frac{\beta}{4t_*}\right)^{1/3} F\left(\frac{1}{2\epsilon}\left(\frac{\beta}{4t_*}\right)^{4/3}\right), \end{aligned}$$

where we have used the change of variable

$$y \to \left(\frac{\beta}{4t_*}\right)^{1/3} z, \tag{4.3}$$

and the function $F(\mu)$ is defined as

$$F(\mu) = \int_{-\infty}^{\infty} e^{\mu(4iz - z^4)} dz. \tag{4.4}$$

Once the zeros $\{\mu_k\}_{k=1}^{\infty}$ of $F(\mu)$ are found, the magnitude β_k of the zeros $\pm i\beta_k$ of $E_\epsilon(i\beta, t_*)$ are given by the relation

$$\beta = \beta_k(t_*, \epsilon) = 4t_*(2\epsilon\mu_k)^{3/4}. \tag{4.5}$$

Thus from (4.2), the zeros of $E_\nu(x,t_*)$ are located at

$$x = \pm a_k(t_*,\nu) = \pm e^{i3\theta/4} i\beta_k(t_*,\epsilon) = \pm e^{i3\theta/4} i4t_*(2\epsilon\mu_k)^{3/4}. \tag{4.6}$$

It is shown in [28] that the k-th ordered large zero μ_k of $F(\mu)$ is given as follows:

PROPERTY 4.1. *Let*

$$\mu_k^{(0)} = \frac{2\pi}{3\sqrt{3}}(k-1/3), \qquad k \geqslant 1,$$

and

$$G(\mu) = \mu + \frac{7}{432\mu}\left(1 - \frac{1}{6\mu}\left(1 + \frac{7}{72\mu}\left(1 - \frac{5}{12\mu}\left(1 + \frac{53143}{18900\mu}\right)\right)\right)\right),$$

then

$$\mu_k = G\left(\mu_k^{(0)}\right) + \mathcal{O}\left(\frac{1}{k^6}\right) \quad \text{as } k \to +\infty.$$

5. Asymptotic analysis of $\Psi_\nu(x,t)$ for $\nu = i\epsilon$, as $\epsilon \to 0^+$, $t > t_*$. When $\nu = i\epsilon$, $\epsilon > 0$, we evaluate the asymptotic behavior of E_ν as $\epsilon \to 0^+$ using the method of stationary phase. We find that all three saddle points are relevant within the caustic $|x| < |x_s(t)| - \delta/2$, where $\delta > 0$ and where $\pm x_s(t)$ are the second order branch points of the inviscid solution (see [29, §6]). For a discussion on such caustics, cf. [23, 26]. When $t > t_*$, $x \in (-\infty, -x_s(t) - \delta/2) \cup (x_s(t) + \delta/2, \infty)$, $\nu = i\epsilon$, $\epsilon \to 0^+$, the same analysis holds and one recovers the characteristic solution outside of the caustic consisting of one relevant saddle point. The transition from within the caustic to outside is not uniform as the asymptotic behavior at the caustic $x = \pm x_s(t)$ is degenerate (2 saddle points have coalesced).

5.1. Asymptotic expansion within the caustic $x \in (-x_s(t)+\delta/2, x_s(t)-\delta/2)$, $\delta > 0$. The caustic $x = x_s(t)$ corresponds to the envelope of the characteristics of the inviscid Burgers solution, and is also determined by the system of equations

$$\begin{cases} 0 = w_z(z,x) = x/t + 2\alpha z - 4z^3, \\ 0 = w_{zz}(z,x) = 2\alpha - 12z^2, \end{cases} \tag{5.1}$$

where $w(z,x)$ is the phase function of the integrand in the definition of $E_\nu(x,t)$. This system represents the conditions for the phase function w to have saddle points of multiplicity two, thereby yielding a curve in the (x,t) plane on which two saddles of multiplicity one coalesce into a saddle of multiplicity two. From the second equation in (5.1), we find $z_{caustic}(t) = \pm\sqrt{\alpha/6}$, and from the first,

$$x = x_{caustic} = t\big(4z_{caustic}(t)^3 - 2\alpha z_{caustic}(t)\big) = \mp t\left(\frac{2\alpha}{3}\right)^{3/2} = \mp x_s(t), \tag{5.2}$$

where $x_s(t) = i\,(3t_*)^{-3/2}(t_* - t)^{3/2}t^{-1/2}$ is the second order branch point of the dispersionless solution described in [29, §6]. Here we are only concerned with the dominant behavior of $E_{i\epsilon}$, thus we only retain the first term:

$$E_{i\epsilon}(x,t) = \sum_{s=0,1,2} \sqrt{\frac{-4\pi i\epsilon}{w_{zz}(z_s,x)}} \exp\left(\frac{w(z_s,x)}{2i\epsilon}\right)\big(1 + \mathcal{O}(\epsilon)\big), \tag{5.3}$$

as $\epsilon \to 0^+$, with

$$w(z_s(x,t),x) = \frac{x}{t} z_s + \alpha z_s^2 - z_s^4 = \frac{3}{4}\frac{x}{t} z_s + \frac{\alpha}{2} z_s^2, \tag{5.4a}$$

$$w_z(z_s(x,t),x) = 0, \quad w_{zz}(z_s(x,t),x) = 2\alpha - 12 z_s^2. \tag{5.4b}$$

The values of the saddle points $z_s = z_s(x,t)$ of (3.6) are determined by the three roots of the first equation in system (5.1), i.e. the first equation of (5.4b). They are specifically

$$\begin{cases} z_0 = \omega \mathcal{A} + \omega^2 \mathcal{B} \\ z_1 = \omega^2 \mathcal{A} + \omega \mathcal{B} \\ z_2 = \mathcal{A} + \mathcal{B} \end{cases} \tag{5.5}$$

with $w = e^{2\pi i/3}$ and

$$\begin{cases} \mathcal{A}(x,t) = (8t)^{-1/3} \cdot \sqrt[3]{x + \sqrt{x^2 - x_s^2}} \\ \mathcal{B}(x,t) = (8t)^{-1/3} \cdot \sqrt[3]{x - \sqrt{x^2 - x_s^2}} \end{cases} \tag{5.6}$$

Note that all three saddle points are real when $x, x_s \in \mathbb{R}$ and the discriminant $\Delta = x^2 - x_s^2 < 0$, that is $|x| < |x_s(t)|$, and in this case $\mathcal{A} = \overline{\mathcal{B}}$ (see [29, Appendix B]). Therefore we have $z_s \in \mathbb{R}$, $w(z_s,x) \in \mathbb{R}$, and $w_{zz}(z_s,x) = 2\alpha - 12 z_s^2 \in \mathbb{R}$. Hence all three terms in the summation signs are oscillatory and equally relevant. Note however that the expansion derived for $E_{i\epsilon}$ is only valid within $|x| < |x_s|$, and in order to get an expansion uniformly valid across $x = \pm x_s$ one needs to derive a uniform expansion as presented in [15, 23]. This analysis is similar in spirit to the one of Jin, Levermore and McLaughlin in [22, §2.2] and that of [15]. The dominant behavior of the solution $\psi_{i\epsilon}(x,t)$ is found from the Cole-Hopf representation, so that within the caustic $|x| < |x_s| - \delta/2$, following the derivation presented in [29, §3], we find

$$\begin{aligned} \Psi_{i\epsilon}(x,t) &= \frac{\sum_{s=0,1,2} z_s \cdot e^{\frac{w(z_s,x)}{2i\epsilon}} / \sqrt{w_{zz}(z_s,x)}}{\sum_{s=0,1,2} e^{\frac{w(z_s,x)}{2i\epsilon}} / \sqrt{w_{zz}(z_s,x)}} + \mathcal{O}(\epsilon) \\ &= \frac{\sum_{s=0,1,2} z_s \cdot e^{\frac{w(z_s,x)}{2i\epsilon} - \frac{i}{2}\arg(w_{zz}(z_s,x))} \cdot |w_{zz}(z_s,x)|^{-1/2}}{\sum_{s=0,1,2} e^{\frac{w(z_s,x)}{2i\epsilon} - \frac{i}{2}\arg(w_{zz}(z_s,x))} \cdot |w_{zz}(z_s,x)|^{-1/2}} + \mathcal{O}(\epsilon). \end{aligned}$$

Since $w_{zz}(z_s,x) \in \mathbb{R}$, we have that $\arg(w_{zz}(z_s,x)) = \frac{\pi}{2}(1 - \mathrm{sgn}(w_{zz}(z_s,x)))$, and therefore the small dispersion behavior of the solution is found from (3.10):

PROPERTY 5.1. *As $\epsilon \to 0^+$ for $x \in (-x_s(t) + \delta/2, x_s(t) - \delta/2)$, $\delta > 0$, $t > t_*$, the spatially singular part of the solution to Burgers' equation is approximated by*

$$\Psi_{i\epsilon}(x,t) = \frac{\sum_{s=0,1,2} z_s \cdot e^{-\frac{i}{2\epsilon} w(z_s,x) + \frac{i\pi}{4} sgn(w_{zz}(z_s,x))} \cdot |w_{zz}(z_s,x)|^{-1/2}}{\sum_{s=0,1,2} e^{-\frac{i}{2\epsilon} w(z_s,x) + \frac{i\pi}{4} sgn(w_{zz}(z_s,x))} \cdot |w_{zz}(z_s,x)|^{-1/2}} + \mathcal{O}(\epsilon).$$

The asymptotic behavior of the solution is then found from the relation

$$\psi_{i\epsilon}(x,t) = \frac{x}{t} - \frac{\Psi_{i\epsilon}(x,t)}{t}.$$

Thus the presence of three competing oscillatory terms in the asymptotic behavior of $\Psi_{i\epsilon}$ is reminiscent of the oscillations observed in the solution $\psi_{i\epsilon}$. Such oscillations are also seen in the pole dynamics in § 7.2.

5.1.1. Long time asymptotics of the stationary phase solution within the caustic. In this section we approximate the stationary phase formula in Property 5.1 for small values of $\delta = x/t$ and find the approximate pole positions for large time. First we claim that the stationary phase formula is valid in a complex neighborhood of $x = 0$ independent of $\epsilon = |\nu|$. A full extension of this formula to the complex plane is difficult to determine because of the possibility of Stokes lines (cf. [26]). Across a Stokes line a stationary point loses its accessibility; i.e. the ability to deform the integration contour to the steepest descent path through the stationary point is lost. The point $x = 0$ does not lie on a Stokes line, however, so that all three stationary points are accessible in a neighborhood of $x = 0$.

Now we can expand the three solutions $y = y_0, y_+, y_-$ of $w_y = 0$, and the corresponding values of w and w_{yy}, in powers of $\delta = x/t$ for fixed value of $\alpha = (t - t_*)/(2tt_*)$ as $\delta \to 0$:

$$
\begin{aligned}
y_0 &= -\frac{\delta}{2\alpha} + \mathcal{O}(\delta^3) \\
y_+ &= \sqrt{\frac{\alpha}{2}} + \frac{\delta}{4\alpha} - \frac{\delta^2}{\alpha^{5/2}}\frac{3}{32\sqrt{2}} + \mathcal{O}(\delta^3) \\
y_- &= -\sqrt{\frac{\alpha}{2}} + \frac{\delta}{4\alpha} + \frac{\delta^2}{\alpha^{5/2}}\frac{3}{32\sqrt{2}} + \mathcal{O}(\delta^3)
\end{aligned} \tag{5.7}
$$

$$
\begin{aligned}
w_0 &= -\frac{\delta^2}{4\alpha} + \mathcal{O}(\delta^3) \\
w_+ &= \frac{\alpha^2}{4} + \delta\sqrt{\frac{\alpha}{2}} + \frac{\delta^2}{8\alpha} + \mathcal{O}(\delta^3) \\
w_- &= \frac{\alpha^2}{4} - \delta\sqrt{\frac{\alpha}{2}} + \frac{\delta^2}{8\alpha} + \mathcal{O}(\delta^3)
\end{aligned} \tag{5.8}
$$

$$
\begin{aligned}
w_{0yy} &= 2\alpha + \mathcal{O}(\delta^2) \\
w_{+yy} &= -4\alpha - 3\delta\sqrt{\frac{2}{\alpha}} + \mathcal{O}(\delta^2) \\
w_{-yy} &= -4\alpha + 3\delta\sqrt{\frac{2}{\alpha}} + \mathcal{O}(\delta^2)
\end{aligned} \tag{5.9}
$$

The stationary phase formula is much more sensitive to the value of w than to the value of w_{yy}, and its leading order form is determined by the terms up to $\mathcal{O}(\delta)$ in w and up to $\mathcal{O}(1)$ in w_{yy}. In particular the leading order form for the denominator D is (for $\nu = i\epsilon$)

$$
\begin{aligned}
D &= \sum_{i=0,+,-} \sqrt{-\frac{\nu}{w_{iyy}}}\, e^{w_i/2\nu} \\
&= \sqrt{\frac{i}{\epsilon}}\left\{ -i|w_{0yy}|^{-1/2} e^{-iw_0/2\epsilon} + |w_{+yy}|^{-1/2} e^{-iw_+/2\epsilon} + |w_{-yy}|^{-1/2} e^{-iw_-/2\epsilon} \right\} \\
&= \frac{1}{2}\sqrt{\frac{i\epsilon}{|\alpha|}}\left\{ -i\sqrt{2} + e^{-w_+/2\epsilon} + e^{-iw_-/2\epsilon} \right\} \\
&= \frac{1}{2}\sqrt{\frac{i\epsilon}{|\alpha|}}\left\{ -i\sqrt{2} + 2\cos\left(\frac{\delta}{2\epsilon}\sqrt{\frac{\alpha}{2}}\right) e^{-i\alpha^2/\delta\epsilon} \right\}.
\end{aligned}
$$

The zeros of D, i.e. the poles for the Burgers solution, are solutions $\delta = x/t$ of the equation

$$\cos\left(\frac{\delta}{2\epsilon}\sqrt{\frac{\alpha}{2}}\right) = \frac{i}{\sqrt{2}} \cdot e^{i\alpha^2/\delta\epsilon}. \tag{5.10}$$

Note that if δ is a solution of (5.10) then so is $-\delta$ and $\delta + \epsilon\alpha_1 n$ with

$$\alpha_1 = 4\pi t\sqrt{\frac{2}{\alpha}}. \tag{5.11}$$

The solutions of (5.10) are

$$\delta = \delta_n^{\pm} = \pm\epsilon\left((x_0 + iy_0)\sqrt{\frac{8}{\alpha}} + n\alpha_1\right) \tag{5.12}$$

and (x_0, y_0) are a particular solution of the equations

$$\sqrt{2}\cos(x_0)\cosh y_0 = -\sin\left(\frac{\alpha^2}{8\epsilon}\right),$$
$$\sqrt{2}\sin(x_0)\sinh y_0 = -\cos\left(\frac{\alpha^2}{8\epsilon}\right).$$

One can easily show that there is a unique solution (x_0, y_0) up to translation and reflection as in (5.12). This shows that to leading order the poles of the dispersive Burgers equation lie on two staggered, horizontal, linear arrays with spacing $\epsilon\alpha_1$.

5.2. $x \in (-x_s(t) - \delta/2, x_s(t) + \delta/2)^c$, $\delta > 0$, $\nu = i\epsilon$, $\epsilon \to 0^+$, $t > t_*$. The inviscid limit is found in a straightforward manner in this case: only one saddle point is relevant, so that the asymptotic limit derived in § 5.1 reduces to

$$\Psi_{i\epsilon}(x,t) = \Psi(x,t) + \mathcal{O}(\epsilon) \qquad \text{as } \epsilon \to 0^+,$$

where $\Psi(x,t) = z_s(x,t)$ is the spatially singular part of the dispersionless solution (see [29, §6]). Thus the solution outside the caustic behaves according to the following property:

PROPERTY 5.2. *As $\nu \to 0^+$ for $x \in (-x_s(t) - \delta/2, x_s(t) + \delta/2)^c$, $\delta > 0$, $t > t_*$, the solution to Burgers' equation is given by*

$$\psi_{i\epsilon}(x,t) = \frac{x}{t} - \frac{\Psi_{i\epsilon}(x,t)}{t} = \frac{x}{t} - \frac{\Psi(x,t)}{t} + \mathcal{O}(\epsilon) \qquad \text{as } \epsilon \to 0^+,$$
$$\Psi(x,t) = z_{s*}(x,t), \quad z_{s*} : \Re w(z_{s*}, x) = \max_{s=0,1,2} \Re w(z_s, x).$$

5.3. Uniform asymptotic expansion across the caustic $x = \pm x_s(t)$ via Pearcey's integral. Following the notation of Kaminski in [23], we introduce the Pearcey integral from which one can derive a uniform asymptotic expansion with two coalescing saddle points: Let

$$P(X,Y) = \int_{-\infty}^{+\infty} e^{i\left(u^4/4 + Xu^2/2 + Yu\right)}\, du \tag{5.13}$$

denote the Pearcey integral. In the arbitrary case $|\theta| \leqslant \pi/2$, one can express $E_{\epsilon e^{i\theta}}(x,t)$ in terms of $P(X,Y)$ defined by (5.14) as:

$$E_{\epsilon e^{i\theta}}(x,t) = \left(\frac{\nu}{2i}\right)^{1/4} P\left(X = -\frac{\alpha}{\sqrt{2\epsilon}} e^{i(\pi/4-\theta/2)}, Y = \frac{-x}{2t}\left(\frac{1}{2\epsilon^3}\right)^{1/4} e^{i(3\pi/8-3\theta/4)}\right).$$

In particular for $\theta = 0$ ($\nu = \epsilon \in \mathbb{R}^+$), we have

$$E_\epsilon(x,t) = \left(\frac{\epsilon}{2i}\right)^{1/4} P\left(X = -\frac{\alpha}{\sqrt{2\epsilon}} e^{i\pi/4}, Y = \frac{-x}{2t}\left(\frac{1}{2\epsilon^3}\right)^{1/4} e^{i3\pi/8}\right).$$

From (3.5), we can express $E_{i\epsilon}(x,t)$ as

$$\begin{aligned} E_{i\epsilon}(x,t) &= \int_{-\infty}^{+\infty} \exp\left\{\frac{i}{2\epsilon}\left(y^4 - \alpha y^2 - \frac{x}{t}y\right)\right\} dy \\ &= \left(\frac{\epsilon}{2}\right)^{1/4} \int_{-\infty}^{+\infty} \exp\left\{i\left(\frac{u^4}{4} - \frac{\alpha}{\sqrt{2\epsilon}}\frac{u^2}{2} - \frac{x}{2t}\left(\frac{1}{2\epsilon^3}\right)^{1/4} u\right)\right\} du \\ &= \left(\frac{\epsilon}{2}\right)^{1/4} P\left(X(\epsilon;t) = \frac{-\alpha}{\sqrt{2\epsilon}}, Y(\epsilon;x,t) = \frac{-x}{2t}\left(\frac{1}{2\epsilon^3}\right)^{1/4}\right). \end{aligned} \tag{5.14}$$

Clearly a small ϵ asymptotic of $E_{i\epsilon}$ is equivalent to a combined asymptotic expansion of the Pearcey integral as $|X|, |Y| \to +\infty$. The caustic of $P(X,Y)$ and the corresponding caustic of $E_{i\epsilon}(x,t)$ is given by

$$Y = \frac{2}{\sqrt{27}} X^{3/2} \iff x = \pm x_s(t). \tag{5.15}$$

Hence the uniform asymptotic behavior of $E_{i\epsilon}$ in a neighborhood of the caustic is found from the one of $P(-X, (2/\sqrt{27} - \tau)X^{3/2})$ as $X \to +\infty$, where $\tau = 0$ at the caustic, and $\tau \neq 0$ away from it (see [23]). This amounts to a uniform expansion valid in $(-|x_s| - \delta(\tau), -|x_s| + \delta(\tau)) \cup (|x_s| - \delta(\tau), |x_s| + \delta(\tau))$ where $\delta(\tau) = \delta(\tau;t) = \frac{\sqrt{27}}{2}|x_s(t)| \cdot \tau \geqslant 0$. Thus it is valid for $|x \pm x_s(t)| \leqslant \delta(\tau;t)$. This expansion is also valid outside of these intervals centered about $\pm x_s(t)$, however the region of interest is the neighborhood of the caustic. Indeed one only needs to use the asymptotic expansion of the Airy function and its derivative to find the results obtained in § 5.1 and 5.2.

From (3.11) and (5.14) we have that

$$\begin{aligned} \Psi_{i\epsilon}(x,t) &= t \cdot 2i\epsilon\, \partial_x \log(E_{i\epsilon}(x,t)) \\ &= t \cdot 2i\epsilon\, \partial_x \log\left[P\left(X(\epsilon;t) = \frac{-\alpha}{\sqrt{2\epsilon}}, Y(\epsilon;x,t) = \frac{-x}{2t}\left(\frac{1}{2\epsilon^3}\right)^{1/4}\right)\right]. \end{aligned}$$

Let

$$X = X(\epsilon;t), \qquad Y = Y(\epsilon;t) = Y(\epsilon; x = -x_s(t) + \delta(\tau;t), t),$$

where $\delta(\tau;t) \to 0^+$ as $\tau \to 0^+$, so that

$$\begin{aligned} \Psi_{i\epsilon}\Big(x = -x_s(t) + \delta(\tau;t), t\Big) &= t \cdot 2i\epsilon\, \partial_x \log\left(P\left(X(\epsilon;t), Y(\epsilon; x = -x_s(t) + \delta(\tau;t), t)\right)\right) \\ &= t \cdot 2i\epsilon\, \partial_\tau \log\left(P\left(-X, (2/\sqrt{27} - \tau)X^{3/2}\right)\right) \Big/ \frac{\partial \delta}{\partial \tau}. \end{aligned}$$

Let $P(\tau) = P\left(-X, (2/\sqrt{27} - \tau)X^{3/2}\right)$, then since $\partial\delta/\partial\tau = \sqrt{27}x_s(t)/2$, we have

$$\Psi_{i\epsilon}\Big(x = -x_s(t) + \delta(\tau;t), t\Big) = \frac{4ti\epsilon}{\sqrt{27}x_s(t)}\frac{P_\tau(\tau)}{P(\tau)}.$$

Following the notation presented in [29], let

$$p_0(\tau) = 3^{-1/6}(1 + \mathcal{O}(\tau)), \quad q_0(\tau) = -\frac{3^{-5/6}}{2}(1 + \mathcal{O}(\tau)), \quad \zeta(\tau) = 3^{-1/6}\tau(1 + \mathcal{O}(\tau)),$$

and

$$f(v) = f(v;\tau) = \frac{v^4}{4} - \frac{v^2}{2} + \left(\frac{2}{\sqrt{27}} - \tau\right)v,$$

and the $v_i, i = 1,2,3$ are the saddle points of $f(v;\tau)$ determined by the equation $f_v(v_i;\tau) = 0$, so that $f(v_i;\tau) = -v_i^2/4 + (2/\sqrt{27} - \tau)3v_i/4$. The v_i's are specifically

$$v_1(\tau) = -\frac{2}{\sqrt{3}}\sin\left(\frac{\pi}{3} + \phi(\tau)\right), \quad v_2(\tau) = \frac{2}{\sqrt{3}}\sin(\phi(\tau)), \quad v_3(\tau) = \frac{2}{\sqrt{3}}\sin\left(\frac{\pi}{3} - \phi(\tau)\right),$$

where

$$\phi = \phi(\tau) = \frac{1}{3}\arcsin\left(1 - \tau\sqrt{27}/2\right), \quad \tau \in \mathbb{R}, \quad |\phi| \leqslant \frac{\pi}{6}.$$

Since

$$X = \frac{-\alpha}{\sqrt{2\epsilon}} \Rightarrow \frac{iX^2}{2} = i\frac{\alpha^2}{4\epsilon} \Rightarrow X^{-2} = \mathcal{O}(\epsilon),$$

then according to the expansion of the Pearcey integral presented by Kaminski [23], we have proved that

PROPERTY 5.3. *The uniform asymptotic expansion as* $\epsilon \to 0^+$ *of* $\Psi_{i\epsilon}(x = -x_s(t) + \delta(\tau;t), t)$ *in a neighborhood of the caustic* $x = -x_s(t)$ *is*

$$\begin{aligned}\Psi_{i\epsilon}\Big(x = -x_s(t) + \delta(\tau;t), t\Big) = \frac{\sqrt{3}}{2}\left(\frac{x_s(t)}{t}\right)^{1/3} \times \Bigg[& [v_2 + v_3]e^{i\frac{\alpha^2}{4\epsilon}[f(v_2)+f(v_3)]} \\ & \times \left\{p_0(\tau)\cdot\frac{2\pi}{X^{1/6}}\cdot Ai(-X^{4/3}\zeta(\tau)) + q_0(\tau)\frac{2\pi}{iX^{5/6}}Ai'(-X^{4/3}\zeta(\tau))\right\} \\ & + 2v_1\, e^{i\frac{\alpha^2}{4\epsilon}2f(v_1)}\left(\frac{\pi}{3v_1^2 - 1}\right)^{1/2}\frac{1+i}{X^{1/2}}\Bigg] \\ \Bigg/ \Bigg[e^{i\frac{\alpha^2}{4\epsilon}[f(v_2)+f(v_3)]} & \cdot \left\{p_0(\tau)\cdot\frac{2\pi}{X^{1/6}}\cdot Ai(-X^{4/3}\zeta(\tau)) + q_0(\tau)\frac{2\pi}{iX^{5/6}}Ai'(-X^{4/3}\zeta(\tau))\right\} \\ & + e^{i\frac{\alpha^2}{4\epsilon}2f(v_1)}\left(\frac{\pi}{3v_1^2 - 1}\right)^{1/2}\frac{1+i}{X^{1/2}}\Bigg] + \mathcal{O}(\epsilon) \quad \text{as } \epsilon \to 0^+.\end{aligned}$$

5.3.1. Behavior at the caustics $x = \pm x_s(t)$. At the caustic $x = -x_s(t)$, $\tau = 0$,

$$\phi(0) = \pi/6, \quad v_1(0) = -2/\sqrt{3}, \quad v_2(0) = v_3(0) = 1/\sqrt{3},$$
$$f(v_i;0) = -v_i^2/4 + v_i/2\sqrt{3}, \quad f(v_2;0) = f(v_3;0) = -2/3, \quad f(v_1;0) = 1/12.$$

Since $X = \mathcal{O}(\epsilon^{-1/2})$, the dominant term as $\epsilon \to 0^+$ in both the numerator and denominator of $\Psi_{i\epsilon}$ is obviously the term containing the factor $X^{-1/6}$. Therefore the dominant behavior of $\Psi_{i\epsilon}(-x_s(t),t)$ reduces to the simple form

$$\begin{aligned}\Psi_{i\epsilon}(-x_s(t),t) &= \frac{\sqrt{3}}{2}\left(\frac{x_s(t)}{t}\right)^{1/3} \cdot (v_2(0) + v_3(0)) + \mathcal{O}(\epsilon) \\ &= \left(\frac{x_s(t)}{t}\right)^{1/3} + \mathcal{O}(\epsilon^{1/3}) \quad \text{as } \epsilon \to 0^+.\end{aligned}$$

6. Continuum limit of the pole expansion and the Calogero dynamical system. From the equation for the pole dynamics and the Mittag-Leffler expansion of the non-zero dispersion solution one can obtain a set of equations for the inviscid limit which give a new representation of the solution to the inviscid burgers equation. Recall the pole expansion

$$\psi_\nu(x,t) = \frac{x}{t} - \sum_{n=1}^{\infty} \frac{4\nu x}{x^2 - a_n^2(t,\nu)} = \frac{x}{t} - 2\nu \sum_{\substack{n=-\infty \\ n\neq 0}}^{\infty} \frac{1}{x - a_n}, \tag{6.1a}$$

and the pole dynamics: $\forall n \in \mathbb{N}^*$,

$$\dot{a}_n = \frac{a_n}{t} - \frac{\nu}{a_n} - 4\nu a_n \sum_{\substack{l=1 \\ l\neq n}}^{\infty} \frac{1}{a_n^2 - a_l^2} = \frac{a_n}{t} - 2\nu \sum_{\substack{l=-\infty \\ l\neq n,0}}^{\infty} \frac{1}{a_n - a_l}. \tag{6.1b}$$

Define the complex map $\mathcal{F}(\zeta,\nu,t)$ as

$$a_n(t,\nu) = \mathcal{F}(\zeta_n^\nu = \nu n, \nu, t) : \mathbb{Z}^* \times \mathbb{R}^+ \times \mathbb{R}^+ \to \mathbb{C}, \qquad a_{-n} = -a_n. \tag{6.2}$$

At t_*, we have (cf. [29, §4.1])

$$\begin{aligned}a_n(t_*,\nu) = \mathcal{F}(\zeta_n^\nu = \nu n, \nu, t_*) &= i \cdot 4t_* \left(2\nu\mu_n\right)^{3/4} \\ &= i \cdot 4t_* \left(2\nu(c_{-1}n + c_0 + c_1/n + \cdots)\right)^{3/4} \\ &= i \cdot 4t_* \left(c_{-1}(2\nu n) + c_0 2\nu + c_1(2\nu)^2/(2\nu n) + \cdots)\right)^{3/4}.\end{aligned}$$

Then introduce the map

$$f(\zeta,t) = \mathcal{F}(\zeta,0,t) : \mathbb{R} \times \mathbb{R}^+ \to \mathbb{C}, \qquad f(-\zeta,t) = -f(\zeta,t), \tag{6.3}$$

where the continuous variable ζ corresponds to a position on the real axis which can be thought of as a variable obtained by simultaneously letting $\nu \to 0^+$ and $n \to +\infty$. Assume that

$$a_n(t,\nu) = \mathcal{F}(n|\nu|,\nu,t) = f(n|\nu|,t) + e_n(t,\nu) \tag{6.4}$$

in which $e_n(t,\nu)$ is a small error term that goes to 0 as $\nu \to 0$. Now let $|\nu| \to 0$ so that $\eta = \nu/|\nu|$ remains constant. Then, at least formally,

$$2\nu \sum_{\ell \neq n} \frac{1}{a_n(t,\nu) - a_\ell(t,\nu)} \simeq 2\eta|\nu| \sum_{\ell \neq n} \frac{1}{f(n|\nu|,t) - f(\ell|\nu|,t)}$$

$$\xrightarrow{\nu \to 0} 2\eta\, P.V. \int_{-\infty}^{\infty} \frac{d\zeta'}{f(\zeta,t) - f(\zeta',t)}. \tag{6.5}$$

Moreover, this approximation shows that the representation (6.4) is valid for all time if it is true at $t = 0$. A rigorous analysis of the approximation (6.5) has been performed in the context of vortex sheets in [9]. A rigorous justification of this limiting process is also presented by other means in [30] for the real viscosity case. It is then clear that the pair of equations (6.1a) and (6.1b) satisfy the following:

PROPERTY 6.1. *The continuum limit of the Calogero dynamical system and the pole expansion is the system of integro-differential equations defined for any x such that $\forall \zeta \in \mathbb{R}$, $x \neq f(\zeta,t)$, by*

$$\frac{\partial f}{\partial t}(\zeta,t) = \frac{f(\zeta,t)}{t} - 2\eta\, P.V. \int_{-\infty}^{\infty} \frac{d\zeta'}{f(\zeta,t) - f(\zeta',t)},$$

$$\psi(x,t) = \frac{x}{t} - 2\eta \int_{-\infty}^{\infty} \frac{d\zeta'}{x - f(\zeta',t)}.$$

This property can also be expressed as

$$\frac{\partial f}{\partial t}(\zeta,t) = \frac{f(\zeta,t)}{t} - 2\eta f(\zeta,t) \int_0^{\infty} \frac{d\zeta'}{f^2(\zeta,t) - f^2(\zeta',t)}$$

$$= \frac{f(\zeta,t)}{t} - \eta f(\zeta,t)\, P.V. \int_{-\infty}^{\infty} \frac{d\zeta'}{f^2(\zeta,t) - f^2(\zeta',t)}, \tag{6.6a}$$

and

$$\psi(x,t) = \frac{x}{t} - 2\eta x \int_0^{\infty} \frac{d\zeta'}{x^2 - f^2(\zeta',t)}$$

$$= \frac{x}{t} - \eta x \int_{-\infty}^{\infty} \frac{d\zeta'}{x^2 - f^2(\zeta',t)}, \qquad x \neq f(\zeta,t). \tag{6.6b}$$

The system consisting of equations (6.6a) and (6.6b) provides a slowly-varying, but incomplete, description of the solution of Burgers' equation and of the pole dynamics: Let $f(\zeta,t)$ solve the continuum (i.e. slowly-varying) equation (6.6a). Then the approximate pole positions are given by (6.4) and the solution ψ_ν of Burgers' equation by the pole expansion (6.1a). Furthermore, as shown in the next subsection, the corresponding solution ψ of the inviscid Burgers' equation is given by (6.6b), and the image of f in $\mathbb{C}$ is a branch cut for ψ. This is an incomplete description, since it does not yield a formula for the wavelength, phase and amplitude of the oscillations. Moreover, when the poles are close to the real line, the oscillations in Burgers' solution are quite sensitive to small errors. In fact, computations presented in § 7.3 for $\nu = \epsilon i$, show that some of the poles found through this "branch cut dynamics" method lie on the real axis, which makes the reconstruction of the solution ψ_ν impossible. We believe that this difficulty could be overcome through improvements in the approximation (6.5).

6.1. Branch cut dynamics. The branch cut dynamics method, presented in this section, is a new method for solving the inviscid Burgers equation

$$\psi_t + \psi\psi_x = 0. \tag{6.7}$$

The main interest here in this method is that it represents the continuum limit, as $|\nu| \to 0$, of the pole dynamics for the viscous equation. It is also interesting to note that the resulting integral-differential equation is nearly the same as the Birkhoff-Rott equation for a vortex sheet, but without the complex conjugation on the right hand side. The branch cut dynamics has a parametric and a non-parametric formulation. In the parametric formulation, the solution is described through the dynamics of a complex-valued function $f(\zeta, t)$ of a real variable ζ. Let $f(\zeta, t)$ satisfy

$$f_t(\zeta, t) = \frac{f(\zeta t)}{t} - 2\eta\, P.V. \int_{-\infty}^{\infty} \frac{d\zeta'}{f(\zeta, t) - f(\zeta', t)} \tag{6.8}$$

in which η is an arbitrary constant. The integral is a Cauchy principal value integral, due to the singularity at $\zeta' = \zeta$, as well as possible singularities at $\zeta' = \pm\infty$. Next define $\psi(x, t)$ by

$$\psi(x, t) = \frac{x}{t} - 2\eta \int_{-\infty}^{\infty} \frac{d\zeta'}{x - f(\zeta', t)}. \tag{6.9}$$

A straightforward calculation shows that $\psi(x, t)$ is a solution to the inviscid Burgers' equation

$$\psi_t + \psi\psi_x = 0 \tag{6.10}$$

for any choice of η. These equations can be rephrased in a second, non-parametric formulation involving a moving curve $\Gamma(t)$ in the complex plane (which may consist of several disconnected parts) and a density function $\rho(z, t)$ defined for $z \in \Gamma(t)$. In particular $\Gamma(t)$ is the image of $f(\zeta, t)$ for ζ varying over the real line. The density function $\rho(z, t)$ is defined by (see [30, §5])

$$\rho(z, t) = \frac{1}{f_\zeta(\zeta, t)}, \tag{6.11}$$

in which $z = f(\zeta, t)$. Then $d\zeta' = \rho(z', t)\, dz'$ and

$$\psi(x, t) = \frac{x}{t} - 2\eta \int_{\Gamma(t)} \frac{\rho(z', t)}{x - z'}\, dz'. \tag{6.12}$$

This formula can be extended into the complex x-plane but is discontinuous across the curve $\Gamma(t)$, i.e. $\Gamma(t)$ is a branch cut for the function ψ. Variations in the arbitrary complex parameter η correspond to variations in the branch cut $\Gamma(t)$ for ψ, without change in the branch point. An application of the Plemejl formulas at a point z on $\Gamma(t)$ shows that limiting values ψ_+ and ψ_- from the right and left, respectively, are

$$\psi_\pm(z, t) = \frac{z}{t} - 2\eta \oint \frac{\rho(z', t)}{z - z'}\, dz' \mp 2\eta\pi i \rho(z, t). \tag{6.13}$$

It follows that the difference of $\psi_\pm$ is

$$\psi_-(z, t) - \psi_+(z, t) = 4\eta\pi i \rho(z, t), \tag{6.14}$$

and the average of $\psi_\pm$ is

$$\begin{aligned}\tilde{\Psi}(z,t) &\equiv \frac{1}{2}(\psi_+(z,t)+\psi_-(z,t)) \\ &= \frac{z}{t} - 2\eta \oint_{\Gamma(t)} \frac{\rho(z',t)}{z-z'}\,dz' \\ &= \frac{x}{t} - 2\eta\, P.V. \int_{-\infty}^{\infty} \frac{d\zeta'}{f(\zeta,t)-f(\zeta',t)} = \frac{\partial f}{\partial t}(\zeta,t). \end{aligned} \tag{6.15}$$

Since $0 = \psi_t + \psi\psi_z = \psi_t + (\frac{1}{2}\psi^2)_z$ for both $\psi = \psi_+$ and ψ_-, it follows that ρ satisfies the conservation equation

$$\rho_t + (\tilde{\Psi}\rho)_z = 0. \tag{6.16}$$

Therefore the branch cut dynamics equations (6.8) and (6.9) are equivalent to the motion of $\Gamma(t)$ by the velocity $\tilde{\Psi}(z,t)$, and the evolution of the density $\rho(z,t)$ through (6.16).

The usefulness of this method in the present context is its relation to the pole dynamics for the viscous (or dispersive) Burgers equation. An interesting equivalent form of the branch cut dynamics equation (6.8) is found by considering the change of time variable

$$\begin{aligned}\tau &= t^{-1} - t_0^{-1} \\ g(\zeta,\tau) &= t^{-1} f(\zeta,t)\end{aligned} \tag{6.17}$$

for any constant t_0. The resulting equation for g is

$$\frac{\partial g}{\partial \tau}(\zeta,\tau) = 2\eta\, P.V. \int_{-\infty}^{\infty} \frac{d\zeta'}{g(\zeta,\tau)-g(\zeta',\tau)}. \tag{6.18}$$

If $\eta = 1/(4\pi i)$, and if the left hand side was replaced by its complex conjugate $\partial\bar{g}/\partial\tau$, this equation would be identical to the Birkhoff-Rott equation for a vortex sheet [9].

7. Numerics. We present numerics which pertain to the analysis previously derived. That is, we use both the stationary phase formula and the pole dynamics as a means to compute the solution. A third method based on a full finite difference scheme is also presented initially. For all three methods, we set the parameter value $t_* = 1$. In all the figures describing the behavior of the solution ψ_ν, we only plot the real part of the solution $\Re\psi_\nu$. Thus whenever there is a label ψ, it should be understood as $\Re\psi_\nu$.

7.1. Finite differences, Runge-Kutta scheme and pole expansion. We present a numerical scheme which enables us to solve (3.1) for arbitrary values of $\arg\nu$ for moderately small values of $|\nu| = \epsilon$. The procedure is sometimes referred to as the method of lines and consists in using a centered difference operator in space while time-marching with a Runge-Kutta scheme. The method is implemented on the interval $I = [0, 1/2]$, with boundary conditions $\psi_\nu(0,t) = 0$ and $\psi_\nu(1/2,t) = 0$. The condition that $\psi_\nu(1/2,t) = 0$ is consistent with the value of the dispersionless solution and as such is consistent for small enough values of ϵ. We can use two different initial conditions:

$$\psi(x,0) = 4x^3 - \frac{x}{t_*} \tag{7.1a}$$

$$\psi_\nu(x,t_*) = \frac{x}{t_*} - 4\nu x \sum_{n=1}^{\infty} \frac{1}{x^2 - a_n^2(t_*,\nu)} \tag{7.1b}$$

If the second condition is used, then the pole positions at $t = t_*$ are specified by the asymptotic estimate presented in (4.1). This estimate is used for all values of μ_n for $10 \leqslant n \leqslant N$:

$$(7.2) \qquad \begin{cases} a_n(t_*,\nu) = e^{i3\theta/4}\, i\, 4t_*(2\epsilon\mu_n)^{3/4}, \\ \mu_n = G(\mu_n^{(0)}), \quad \mu_n^{(0)} = \frac{2\pi}{3\sqrt{3}}(n-1/3), \quad n \geqslant 10, \\ G(\mu) = \mu + \frac{7}{432\mu}\left(1 - \frac{1}{6\mu}\left(1 + \frac{7}{72\mu}\left(1 - \frac{5}{12\mu}\left(1 + \frac{53143}{18900\mu}\right)\right)\right)\right), \end{cases}$$

For $1 \leqslant n \leqslant 9$, we use the numerical values found in [28, Table 3], under the column "Numerical roots":

$$\begin{aligned} &\mu_1 = 0.8221037147 \quad \mu_2 = 2.0226889660 \quad \mu_3 = 3.2292915284 \\ &\mu_4 = 4.4372464748 \quad \mu_5 = 5.6457167459 \quad \mu_6 = 6.8544374340 \\ &\mu_7 = 8.0632985369 \quad \mu_8 = 9.2722462225 \quad \mu_9 = 10.4812510479. \end{aligned}$$

Let

$$\begin{aligned} &\psi_j = \psi(j*\Delta x, t), \quad E\psi_j = \psi_{j+1}, \quad E^p\psi_j = \psi_{j+p}, \\ &D_+ = (E - E^0)/\Delta x, \quad D_- = (E^0 - E^{-1})/\Delta x, \quad D_0 = (D_+ + D_-)/2. \end{aligned}$$

One then solves the system of J equations using a Runge-Kutta 4-5 scheme:

$$(7.3) \qquad \frac{d\psi_j}{dt} = -D_0(\psi_j^2/2) + \nu D_+ D_- \psi_j, \qquad j = 1, \cdots, J,$$

where $J * \Delta x = 1/2$, $\psi_{j=0} = 0$ and $\psi_J = 0$.

7.2. Numerical pole dynamics. We now investigate the motion of the simple poles of $\psi_\nu(x,t)$ for various values of $\nu \in \mathbb{C}^+$. The procedure consists in truncating the Calogero dynamical system and by starting with initial data for the poles at $t = t_*$: the complex poles of $\psi_\nu(x,t)$ are located at $x = \pm a_n(t,\nu) = \pm\sqrt{\nu\kappa_n(t,\nu)}$, where the variables κ_n satisfy the system

$$(7.4) \qquad \forall n \in \mathbb{N}^*, \quad \begin{cases} \frac{1}{2}\frac{d\kappa_n}{dt} = \frac{\kappa_n}{t} - 1 - 4\,\kappa_n \sum_{\substack{l=1 \\ l\neq n}}^{\infty} \frac{1}{\kappa_n - \kappa_l} \\ \kappa_n(t_*,\nu) = a_n^2(t_*,\nu)/\nu. \end{cases}$$

$a_n(t_*,\nu)$ is computed as is described in the previous section. The value of $a_n(t,\nu)$ is recovered using the relation $a_n(t,\nu) = \sqrt{\nu\kappa_n(t,\nu)}$. Starting from $t = t_*$, we compute and plot the evolution of the first four poles $a_n(t,\nu), n = -4, \cdots, 4$ for different values of ν. We use N poles in the computations, i.e. a_1 through a_N where $N \times 10^{-4}$ is either $1, 2.5, 5, 10$. That is, we consider the truncated system

$$\forall n = 1, \cdots, N, \quad \begin{cases} \frac{\dot\kappa_n}{2} = \frac{\kappa_n}{t} - 1 - 4\kappa_n \sum_{\substack{l=1 \\ l\neq n}}^{N} \frac{1}{\kappa_n - \kappa_l} \\ \kappa_n(t_*,\nu) = (4t_*)^2(2\mu_n)^{3/2}\sqrt{\epsilon}e^{i\theta/2} \end{cases}$$

where the integer N is appropriately chosen. In order to accelerate the computation of the slowly converging pole expansions

$$\sum_{\substack{l=1 \\ l\neq n}}^{N} \frac{1}{\kappa_l - \kappa_n}, \qquad \forall n = 1, \cdots, N$$

we use the Multipole algorithm developed by Greengard and Rokhlin (see [20]) and implemented by Greengard, which reduces the number of operations from $\mathcal{O}(N^2)$ to $\mathcal{O}(N \log N)$. A fourth/fifth order Runge-Kutta-Fehlberg scheme with automatic step-size control is used. Since the initial data is specified at $t = t_* = 1$, we can solve the system forward and backwards in time starting from $t = 1$. The typical tolerance in the computation is $10^{-8} < |\frac{x_4 - x_5}{x_5}| < 10^{-4}$ where x_4 and x_5 are respectively the fourth and fifth order estimates of $\kappa_1(t,\nu)$. Once the tolerance criterion is met, we recover the pole location via the relation $a_n(t,\nu) = \sqrt{\nu \kappa_n(t,\nu)}$. The difference between the complex ν case and the real ν case is that the variables are all real for ν real, thus system (7.4) is a system of real ODEs, whereas for $\nu \in \mathbb{C}^+$, system (7.4) is a genuinely complex ODE system. The justification of the numerics is the most difficult aspect of this simulation because one must justify the convergence of the method both as the number of poles increases and as the time step is refined. The time-step control is automatically determined by the relative tolerance (R.T.) test on the 4-th and 5-th order approximations of the first ordered pole (the one closest to the origin). Thus one cannot fix the time stepping, rather one can have a subtle control on it by reducing this tolerance. Typically, we fix the number of poles to 50,000 and vary the tolerance on the successive intervals $10^{-10} < R.T. < 10^{-6}$, $10^{-8} < R.T. < 10^{-4}$, $10^{-6} < R.T. < 10^{-2}$. Then we fix the tolerance at the highest reasonable level $10^{-8} < R.T. < 10^{-4}$, and vary the number of poles where $N \times 10^{-4}$ varies from $1, 2.5, 5, 10$. Another test of accuracy is performed on an exactly solvable 2-pair pole dynamics (see [29, §5]). A discussion of the convergence of the pole dynamics method for the case $\nu \in \mathbb{R}$ can be found in [29]. The convergence of the (truncated) pole dynamics to the true solution of the (infinite) Calogero dynamical system as the number of poles N increases and as the time stepping of the Runge-Kutta scheme is decreased improves as the argument θ of ν increases to $\pi/2$, and worsens as the magnitude ϵ of ν decreases. The convergence improves with increasing θ because the position of the poles at t_* gets closer to the real axis. The closer the poles are to the real axis, the better the convergence in the tails of the solution becomes. Indeed, the most difficult case (computationally) occurs when $\arg \nu = 0$, as discussed in [29].

When $\nu > 0$, the behavior of the pole $\beta_1(t,\nu)$ displayed in [29] describes the evolution of the width of the analyticity strip of the viscous solution (see [29]).

When $\nu \in i\mathbb{R}$, the behavior of the poles is studied as $\epsilon = |\nu|$ decreases to 0. One can observe a structuring of the pole behavior into a spiraling motion at the end of which they end close to the real axis for $t \approx t_*, t > t_*$. It is the presence of these poles close to the real axis which gives rise to rapid oscillations which are observed both in the pole expansion reconstruction and the stationary phase approximation. We describe many cases for ϵ ranging from $\epsilon = 10^{-2}$ to $\epsilon = 10^{-5}$ due to the drastic difference in the behavior of the poles displayed in Figs. B.1, B.2, B.5, B.6, B.11, B.15. In many of these figures, we do not display the full height of the oscillations in order to compare the pole dynamics with the stationary phase approximation. The agreement between the two methods is remarkable (Figs. B.9, B.14, B.17). The few discrepencies which can be observed in these figures occur in the amplitude of the peaks of certain oscillations. They are due to the extreme sensitivity of the pole reconstruction to the pole positions. The accuracy of the match between the stationary phase approximation and the pole dynamics also serves as a justification for the pole dynamics.

Finally, only the case $\epsilon = 10^{-3}$ is treated for $\arg \nu = \pi/4$ to illustrate the behavior of a mixed dissipative-dispersive system (see (3.3)). In this case ($\arg \nu = \pi/4$), the di-

versity in the behavior of the poles is much less rich than that observed for $\arg\nu = \pi/2$. Moreover, the number of oscillations is fixed to one, and as such is less interesting to observe. However it is included to provide a comparison with the (full) finite difference scheme (method of lines).

7.3. Numerical branch cut dynamics. Finally we present the results of numerical computations for the branch cut dynamics equation. Rather than solving (6.8) directly, we move points $X(t)$ on the branch cut through the equation

$$\dot{X}(t) = \frac{1}{2}(\psi_+ + \psi_-)(X(t), t), \tag{7.5}$$

in which ψ_+ and ψ_- are the limits from the right and left, respectively, of the corresponding solution of the inviscid Burgers equation. For the initial data $\psi(x,0) = 4x^3 - x/t_*$, the positions of the poles are prescribed at $t = t_*$ to be the pole positions for Burgers equation with viscosity $\nu = \epsilon e^{i\theta}$, as described in § 4 and [28]. In particular they lie on the line $\arg(z) = 3\theta/4$. Their location for $t > t_*$ is found by solving the ODE (7.5). Moreover the solution values

$$\psi(x,t) = \psi_0(x_0) = 4x_0^3 - x_0/t_* \tag{7.6}$$

are found through the inversion of the cubic equation (see [29, §6])

$$x = x_0 + t\,\psi_0(x_0) = 4tx_0^3 + x_0(t_* - t)/t_*. \tag{7.7}$$

At a complex point x on the branch cut we have

$$\psi_+(x,t) = \psi_0(x_+(x,t),t), \qquad \psi_-(x,t) = \psi_0(x_-(x,t),t), \tag{7.8}$$

in which x_+ and x_- are the limiting values of x_0 from the right and left at the point x. For large positive or negative values of x on the real line, the cubic equation (7.7) has a single real value $x_0 = x_0(x,t)$. The value $x_+(x,t)$ is the analytic continuation of this real value of $x_0(x,t)$ from the positive real axis; the value $x_-(x,t)$ is the analytic continuation of $x_0(x,t)$ from the negative real axis.

Results of numerical solution of the branch cut dynamics equation in the form (7.5) corresponding to initial data (7.6) are presented in Figs. B.4, B.8, B.13, B.20, for $\nu = 10^{-5}i$, $10^{-4}i$, $10^{-3}i$ and $10^{-3}\sqrt{i}$. As described in § 6.1, the equation for the branch cut depends only on $\theta = \arg(\nu)$; the value of ϵ is only used to determine the positions of the poles at $t = t_*$ corresponding to that value of ν. In each of these figures, as well as in similar computations for other values of ν, we see that the branch cut is a line of angle $3\theta/4$ at $t = t_*$, and that as t increases, the branch cut again approaches a line but with a small angle. For $\theta = \pi/2$ (i.e. $\nu = \epsilon i$) the branch cut moves onto the real line as t increases.

Next we compare the pole positions computed by the branch cut dynamics method with those obtained from the Calogero equations. The Calogero system is exact, except for discretization in t and a cutoff in the number N of poles. In the case $\nu = 10^{-3}\sqrt{i}$, there is excellent agreement between the results from the branch cut dynamics (Fig. B.20) and those from the Calogero system (Fig. B.19). The cases with $\nu = \epsilon i$ are more interesting, since there are oscillations in the corresponding Burgers' solution. The branch cut dynamics results of Figs. B.4, B.8, B.13 are in excellent agreement with the Calogero results of Figs. B.3, B.7, B.12 for poles that are outside the caustic

points of the inviscid Burgers solution. Within the caustic region, the poles from the branch cut dynamics lie on the real axis, while those from Calogero lie slightly off. On the other hand, the real parts of the pole positions from the two methods are in good agreement.

This shows that the branch cut dynamics does a very good job of describing the pole dynamics for Burgers equation with complex viscosity, except within the caustic region for imaginary viscosity.

A. Generalization of the initial data to $\psi_0(x) = 2nx^{2n-1} - x/t_*$. Using a result in [29] concerning the asymptotic behavior of the k-th zero $\mu_{k,n}$ of $\mathcal{F}_n(\mu) = \int_{-\infty}^{\infty} e^{\mu(2niz - z^{2n})} dz$, we can prove the following:

PROPERTY A.1. *Let $n \in \mathbb{N}$, $n \geqslant 2$, and let $\nu = \epsilon e^{i\theta} \in \mathbb{C}^+ = \{\epsilon > 0, |\theta| \leqslant \pi/2\}$. The $k-th$ ordered pole of the solution at $t = t_*$ arising from the initial data $\psi_0(x) = 2nx^{2n-1} - x/t_*$ is located at*

$$a_{k,n}(t_*, \nu = \epsilon e^{i\theta}) = e^{i\frac{2n-1}{2n}\theta} i \cdot 2nt_* \left(2\epsilon\mu_{k,n}\right)^{\frac{2n-1}{2n}},$$

where the coefficients $\mu_{k,n}$ are asymptotically given by

$$\mu_{k,n} = \frac{\pi}{4n-2} \sec\left(\frac{\pi}{4n-2}\right)\left(\frac{n-1}{2n-1} + 1 + 2k\right) + \mathcal{O}\left(\frac{1}{k}\right) \quad \text{as } k \to +\infty.$$

Acknowledgment. The first author gratefully acknowledges Prof. L. Greengard for the expeditious use of his Multipole code which greatly enhanced the study of the numerical pole dynamics, and Dr. Anders Peterson for many valuable conversations concerning the method of lines.

REFERENCES

[1] M. ABRAMOWITZ AND I.A. STEGUN, *Handbook of Mathematical Functions*, 1964.
[2] L.V. AHLFORS, *Complex Analysis*, Mc.Graw Hill, 3rd. edition, 1979.
[3] D. BESSIS AND J.D. FOURNIER, *Complex singularities and the Riemann surface for the Burgers equation*, Research Reports in Physics - Nonlinear Physics, Springer-Verlag Berlin, Heidelberg 1990, pp. 252-257.
[4] D. BESSIS AND J.D. FOURNIER, *Pole condensation and the Riemann surface associated with a shock in Burgers equation*, J.Phys.Lett. **45** (1984), L833-L841.
[5] R.P. BOAS, *Entire Functions*, Academic Press Inc., 1954.
[6] J.M. BURGERS, *A mathematical model illustrating the theory of turbulence*, Adv. Appl. Mech., Vol **1** (1948), pp. 171-199.
[7] J.M. BURGERS, *The Nonlinear Diffusion Equation*, D. Reidel Publishing Co., 1974.
[8] R.E. CAFLISCH, N. ERCOLANI, T.Y. HOU AND Y. LANDIS, *Multi-valued solutions and branch point singularities for nonlinear hyperbolic or elliptic systems*, Comm. Pure Appl. Math. **46** (1993), pp. 453-499.
[9] R.E. CAFLISCH AND J.S. LOWENGRUB, *Convergence of the Vortex Method for Vortex Sheets*, SIAM J. Num. Anal. **26** (1989), pp. 1060-1080.
[10] F. CALOGERO, *Motion of poles and zeros of special solutions of nonlinear and linear partial differential equations and related "solvable" many body problems*, Il Nuovo Cimento **43B** No. 2 (1978), pp. 177-241.
[11] D.V. CHOODNOVSKY AND G.V. CHOODNOVSKY, *Pole expansions of nonlinear partial differential equations*, Il Nuovo Cimento **40B** No. 2 (1977), pp. 339-353.
[12] J.D. COLE, *On a quasi-linear parabolic equation occuring in aerodynamics*, Quart. Appl. Math. **9** (1951), pp. 225-236.
[13] E.T. COPSON, *Asymptotic Expansions*, Cambridge University Press, 1965.

[14] E.T. COPSON, *An Introduction to the Theory of Functions of a Complex Variable*, Oxford University Press, 1957.

[15] S.Y. DOBROKHOTOV, V.P. MASLOV AND V.B. TSVETKOV, *Problem of the reversal of a wave for the model equation* $v_t + vv_x - \frac{ih}{2} v_{xx} = 0$, Matematicheskie Zametki, Vol. **51**, No. 6 (1992), pp. 143-147.

[16] N.M. ERCOLANI, I.R. GABITOV, C.D. LEVERMORE AND D. SERRE eds., *Singular Limits of Dispersive Waves*, NATO ASI Series, Series B. Physics Vol. **320**, 1994.

[17] N.M. ERCOLANI, C.D. LEVERMORE AND T. ZHANG, *The behavior of the Weyl function in the zero-dispersion KdV limit*, MSRI Preprint No. 045-94, 1994 (to appear in Comm. Math. Phys.).

[18] J.D. FOURNIER AND U. FRISCH, *L'équation de Burgers deterministe et statistique*, J. Mec. Th. Appl. **2** (1983), pp. 699-750.

[19] U. FRISCH AND R. MORF, *Intermittency in nonlinear dynamics and singularitites at complex times*, Phys. Rev. A **23**, No. 5 (1981), pp. 2673-2705.

[20] L. GREENGARD AND V. ROKHLIN, *A fast algorithm for particle simulations*, J. Comp. Phys. **73** (1987), pp. 325-348.

[21] E. HOPF, *The partial differential equation* $u_t + u\, u_x = \mu\, u_{xx}$, Comm. Pure Appl. Math. **3** (1950), pp. 201-230.

[22] S. JIN, C.D. LEVERMORE AND D.W. MCLAUGHLIN, *The behavior of solutions of the NLS equation in the semiclassical limit*, pp. 235-255, Singular Limits of Dispersive waves, edited by N.M. Ercolani et al., Plenum Press, New York, 1994.

[23] D. KAMINSKI, *Asymptotic expansion of the Pearcey integral near the caustic*, SIAM J. Math. Anal., **20** (1989), pp. 987-1005.

[24] P.D. LAX AND C.D. LEVERMORE, *The small dispersion limit of the Korteweg de Vries equation*, I, II, III, Comm. Pure Appl. Math. **36** (1983), pp. 253-290, pp. 571-593, pp. 809-829.

[25] C.D. LEVERMORE AND J.G. LIU, *Oscillations arising in numerical experiments*, in Singular Limits of Dispersive waves, edited by N.M. Ercolani et al., Plenum Press, New York, 1994, pp. 329-346.

[26] R.B. PARIS, *The asymptotic behavior of Pearcey's integral for complex variables*, Proc. Roy. Soc. London, Ser. A **432** (1991), pp. 391-426.

[27] G. PÓLYA, *Über trigonometrische integrale mit nur reellen nullstellen*, Journal für die reine und angewandte Mathematik **158** (1927), pp. 6-18.

[28] D. SENOUF, *Asymptotic and numerical approximations of the zeros of Fourier integrals*, to appear in SIAM J. Math. Anal.

[29] D. SENOUF, *On the real time dynamics of complex singularities for Burgers' equation*, submitted to SIAM J. Math. Anal.

[30] D. SENOUF, *On the zero-viscosity limit of Burgers' equation from the perspective of complex singularities*, submitted to SIAM J. Math. Anal.

[31] C. SULEM, P.L. SULEM AND H. FRISCH, *Tracing complex singularities with spectral methods*, J. Comp. Phys. **50** (1983), pp. 138-161.

[32] O. THUAL, U. FRISCH AND M. HÉNON, *Application of pole decomposition to an equation governing the dynamics of wrinkled flame fronts*, J. Phys. **46** (1985), pp. 1485-1494.

[33] F. URSELL, *Integrals with a large parameter. Several nearly coincident saddle points*, Proc. Cambridge Phil. Soc., **72** (1972), pp. 49-65.

[34] G.B. WHITHAM, *Linear and Nonlinear Waves*, Wiley Interscience, 1974.

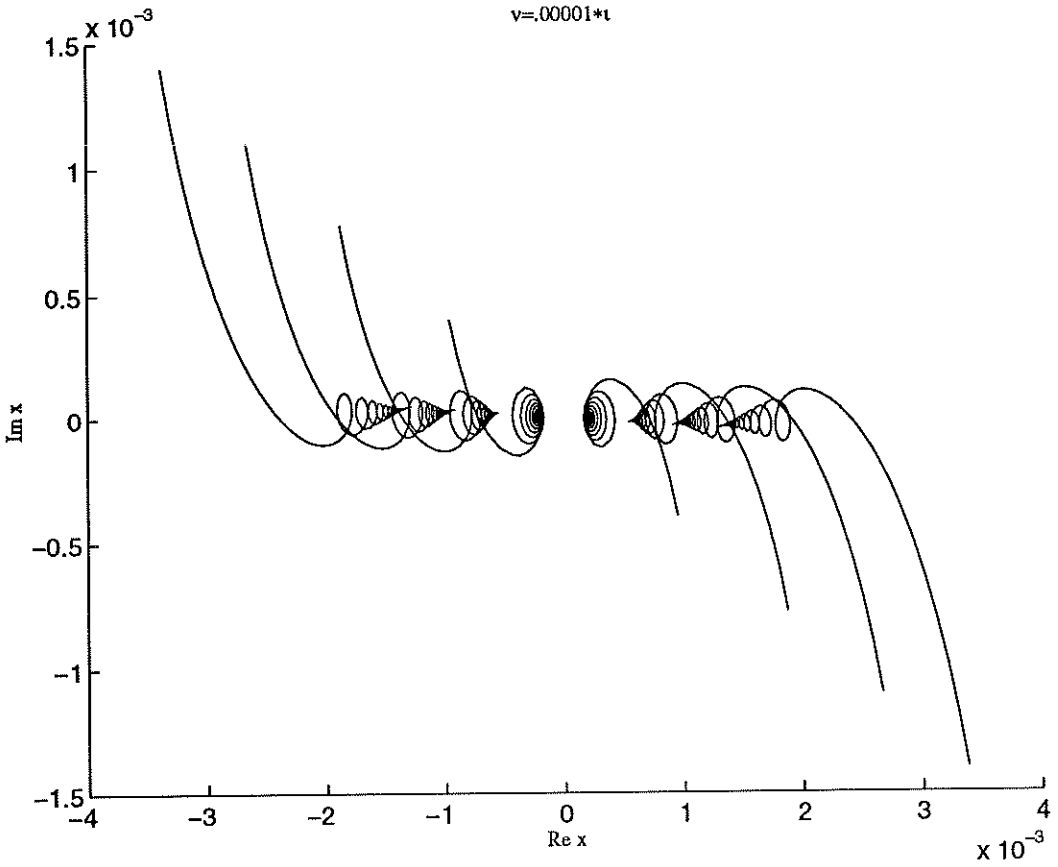

FIG. B.1. $\Im\, a_j(t,\nu)$ *vs.* $\Re\, a_j(t,\nu)$. *Time evolution in* $\mathbb{C}$ *of* $a_j(t,\nu)$, $j=-4,\cdots,4$ *for* $\nu = 10^{-5}\times i$ *and* $N(numberofpoles) = 10^5$. $t_{initial} = t_* = 1$ *and* $t_{final} = 1.25$. *Typical timestep* $\delta t \approx 10^{-3}$. $n_{steps} = 175$. *Time stepping tolerance* $10^{-8} < L.R.T < 10^{-4}$.

Figures.

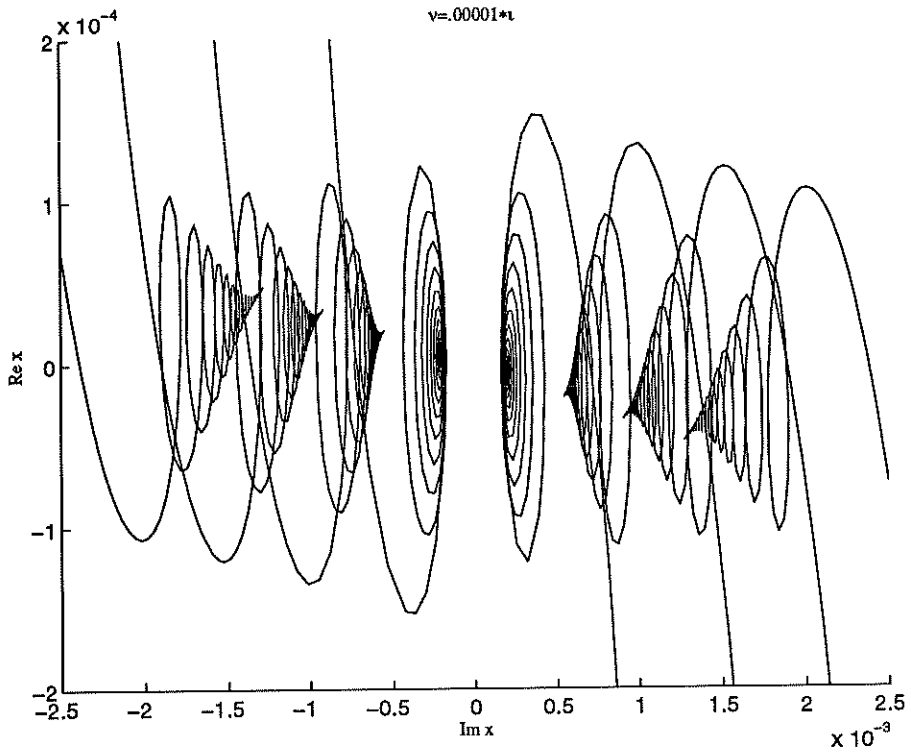

FIG. B.2. *Closeup of Figure B.1.*

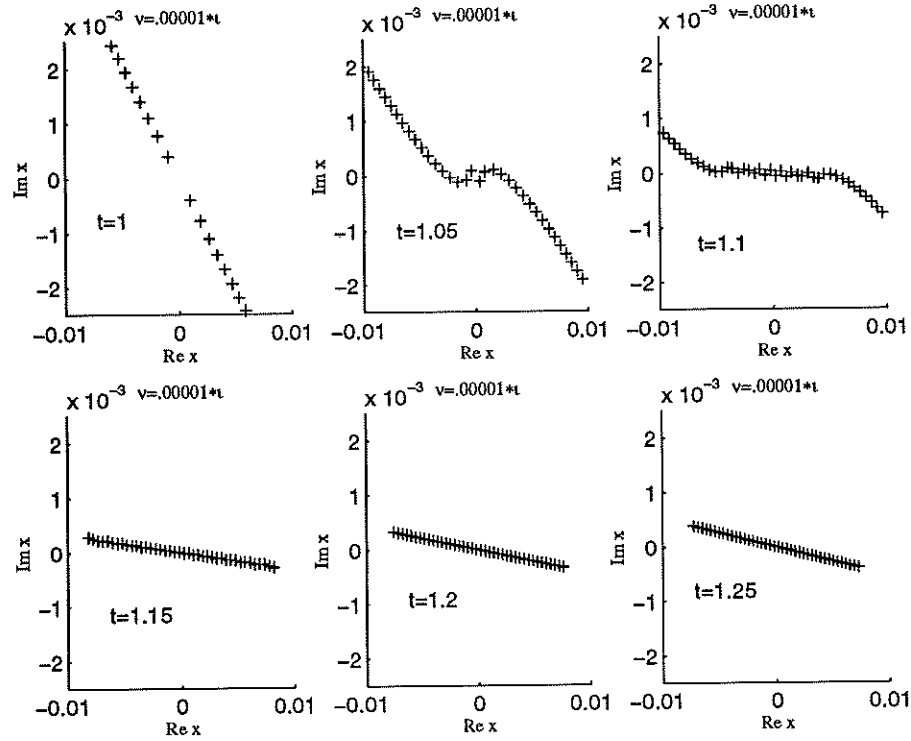

FIG. B.3. *Positions of the first 20 poles from the pole dynamics for* $\nu = 10^{-5} \times i$ *and* $N = 10^5$ *at* $t = 1, 1.05, 1.1, 1.15, 1.2, 1.25$.

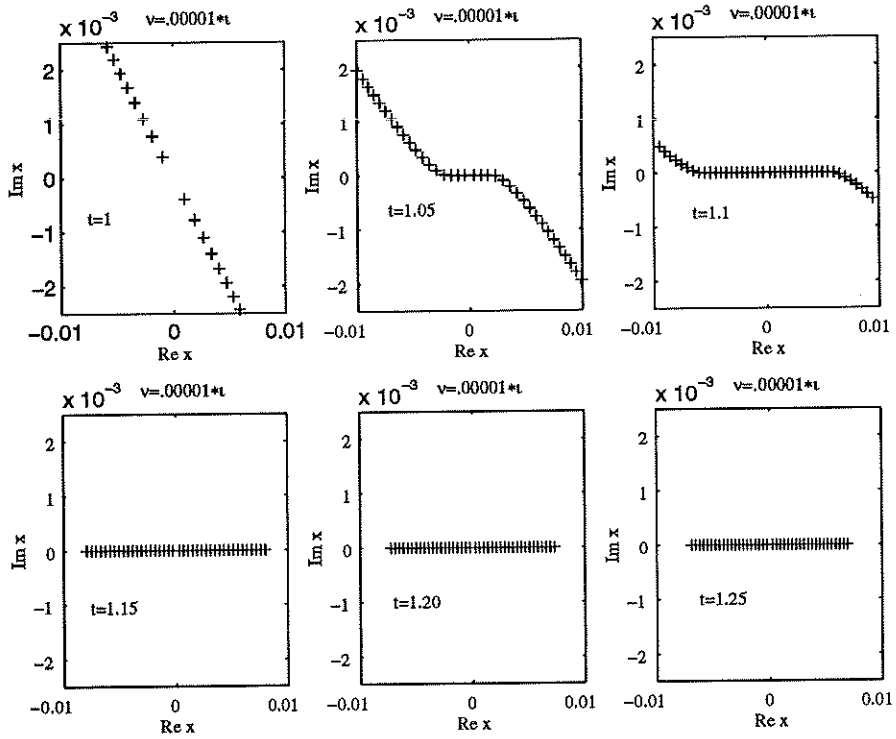

FIG. B.4. *Branch cut dynamics for* $\nu = 10^{-5} \times i$ *at* $t = 1, 1.05, 1.1, 1.15, 1.2, 1.25$.

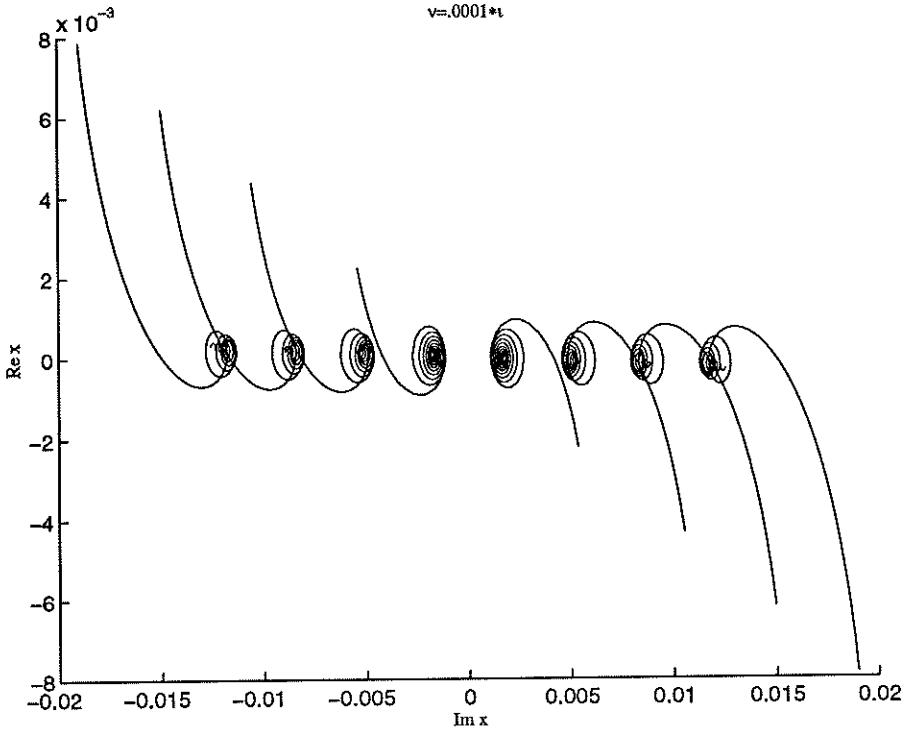

FIG. B.5. $\Im a_j(t,\nu)$ *vs.* $\Re a_j(t,\nu)$. *Time evolution in* $\mathbb{C}$ *of* $a_j(t,\nu)$, $j = -4, \cdots, 4$ *for* $\nu = 10^{-4} \times i$ *and* $N = 10^5$. $t_{initial} = t_* = 1$ *and* $t_{final} = 2$. $n_{steps} = 280$. *Typical timestep* $\delta t \approx 3 \times 10^{-3}$. *Time stepping tolerance:* $10^{-8} < L.R.T < 10^{-4}$.

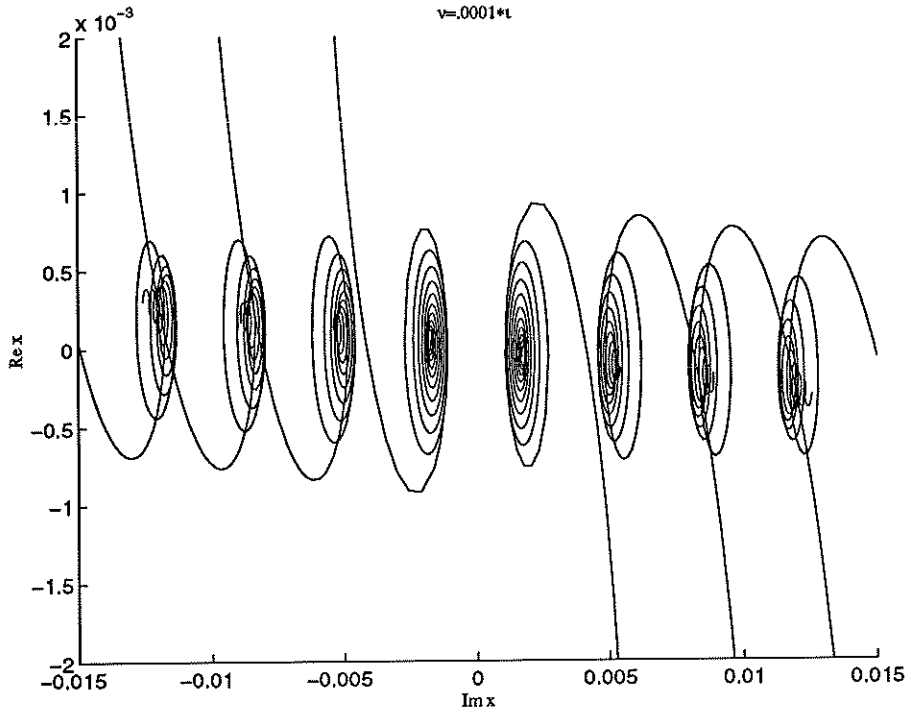

FIG. B.6. *Close-up of Fig. B.5.*

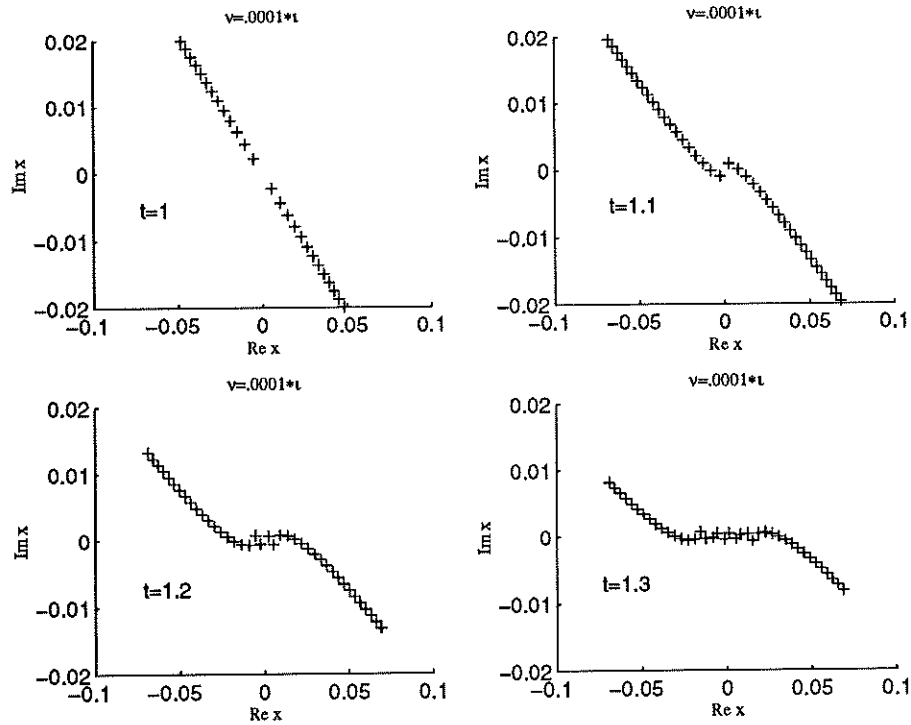

FIG. B.7. *Positions of the first 20 poles from the pole dynamics for* $\nu = 10^{-4} \times i$ *and* $N = 10^5$ *at* $t = 1, 1.1, 1.2, 1.3$.

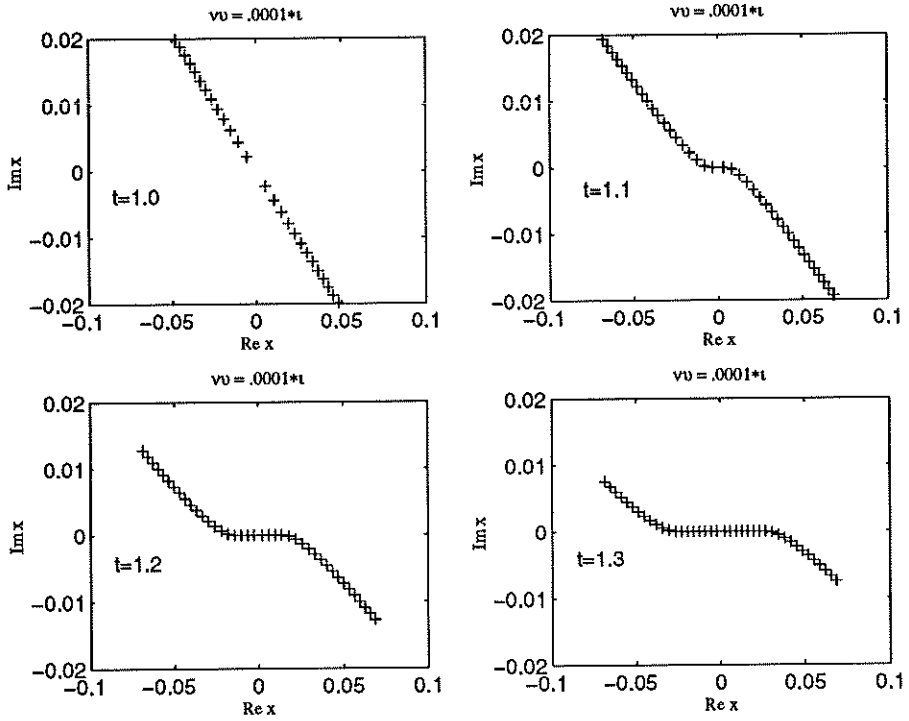

FIG. B.8. *Branch cut dynamics for* $\nu = 10^{-4} \times i$ *at* $t = 1, 1.1, 1.2, 1.3$.

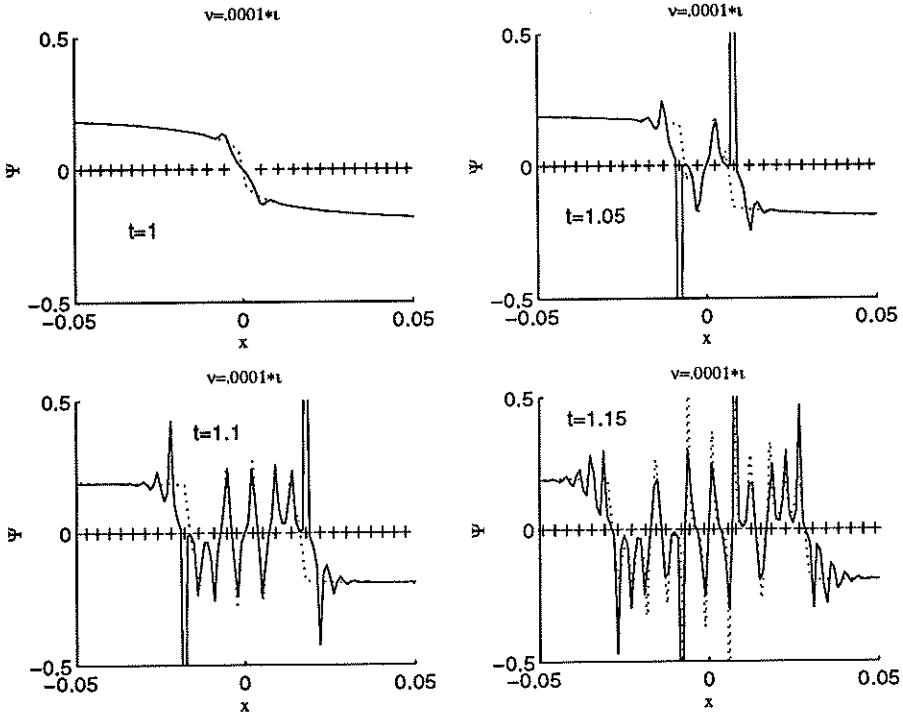

FIG. B.9. $\Re\psi_\nu(x,t)$ *vs.* x *from the pole dynamics for* $\nu = 10^{-4} \times i$ *and* $N = 10^5$ *at* $t = 1, 1.05, 1.1, 1.15$.

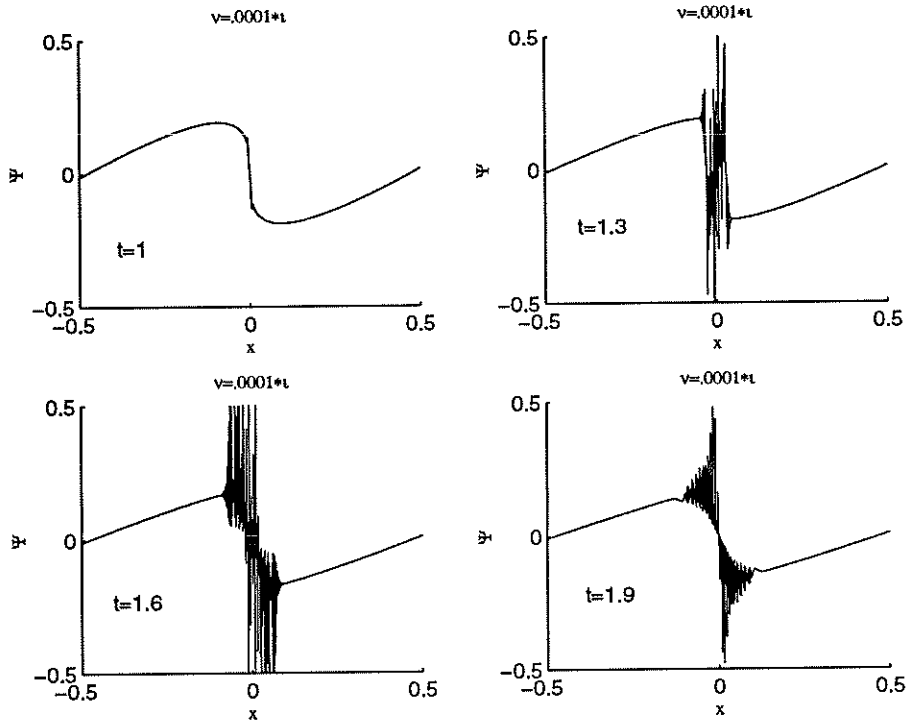

FIG. B.10. $\Re\psi_\nu(x,t)$ *vs.* x *from the pole dynamics for* $\nu = 10^{-4} \times i$ *and* $N = 10^5$ *at* $t = 1, 1.3, 1.6, 1.9$.

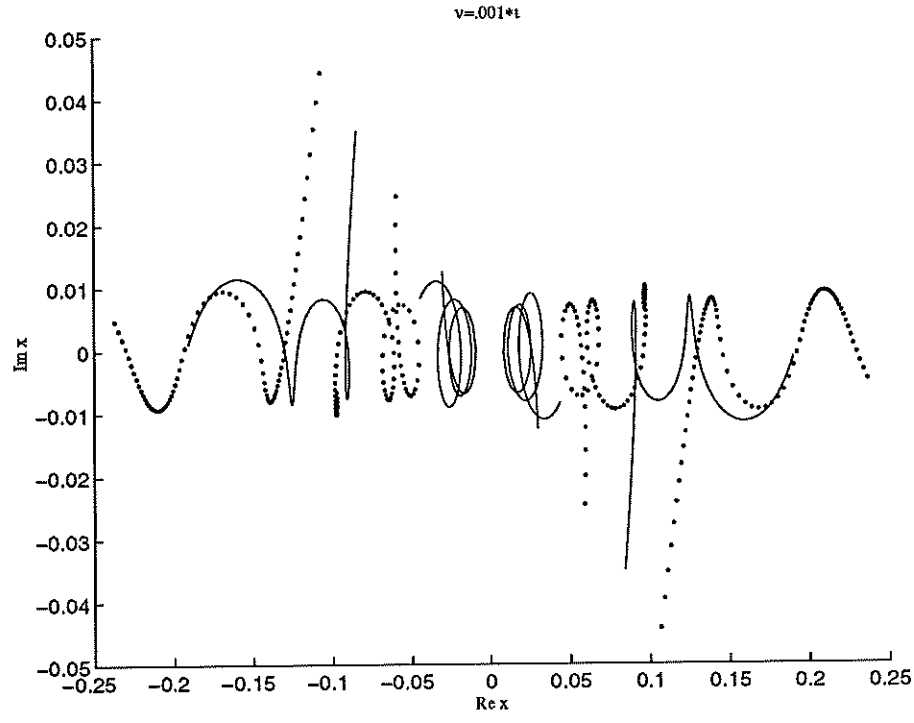

FIG. B.11. $\Im a_j(t,\nu)$ *vs.* $\Re a_j(t,\nu)$. *Time evolution in* $\mathbb{C}$ *of* $a_j(t,\nu)$, $j = -4, \cdots, 4$ *for* $\nu = 10^{-3} \times i$ *and* $N = 10^5$. $t_{initial} = t_* = 1$ *and* $t_{final} = 4$. $n_{steps} = 80$. *Typical timestep* $\delta t = .05$. *Time stepping tolerance:* $10^{-8} < L.R.T < 10^{-4}$.

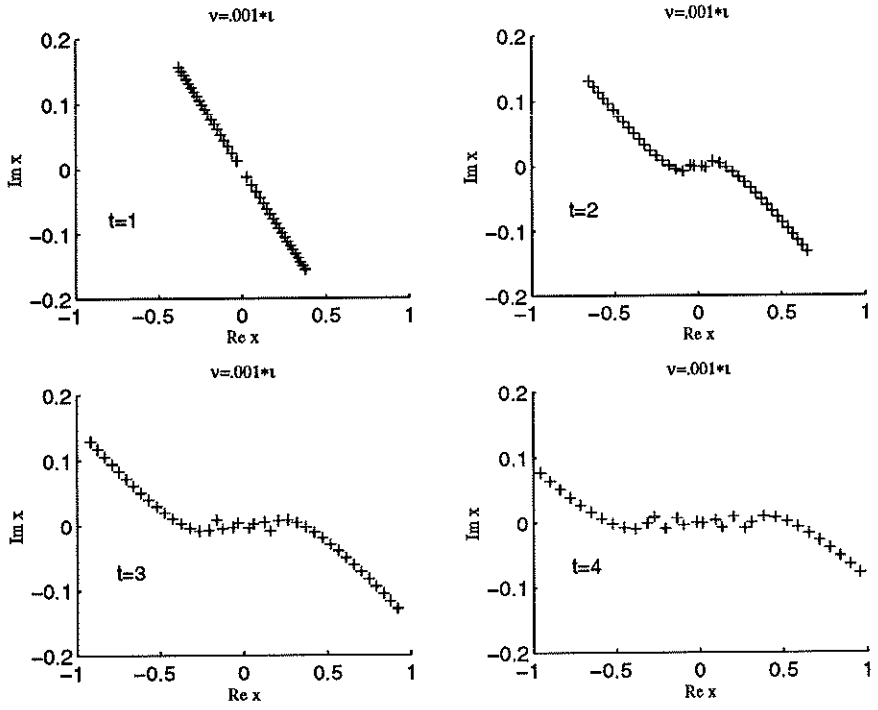

FIG. B.12. *Positions of the first 20 poles from the pole dynamics for* $\nu = 10^{-3} \times i$ *and* $N = 10^5$ *at* $t = 1, 2, 3, 4$.

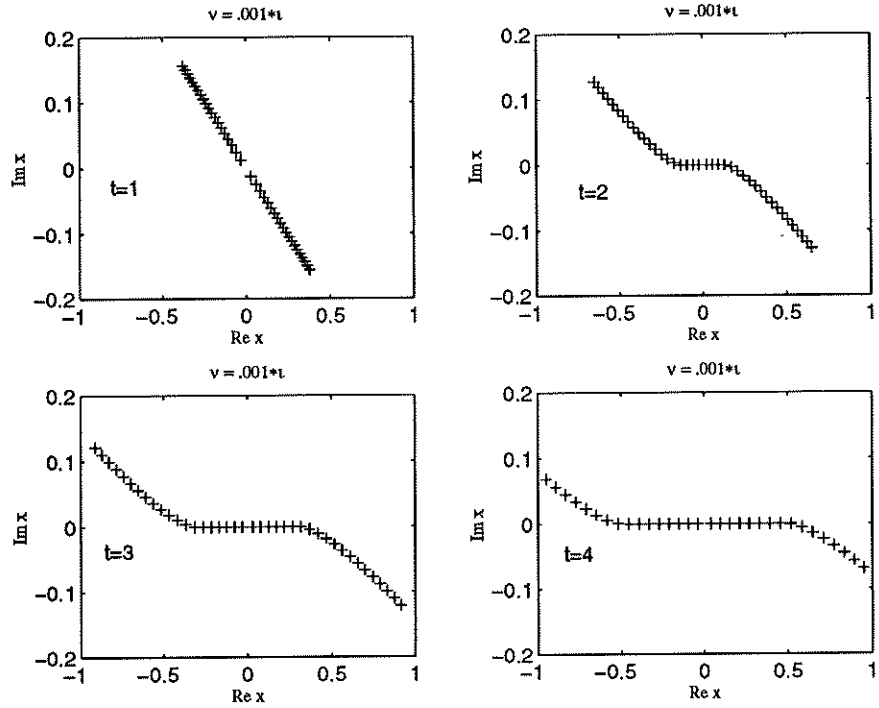

FIG. B.13. *Branch cut dynamics for* $\nu = 10^{-3} \times i$ *at* $t = 1, 2, 3, 4$.

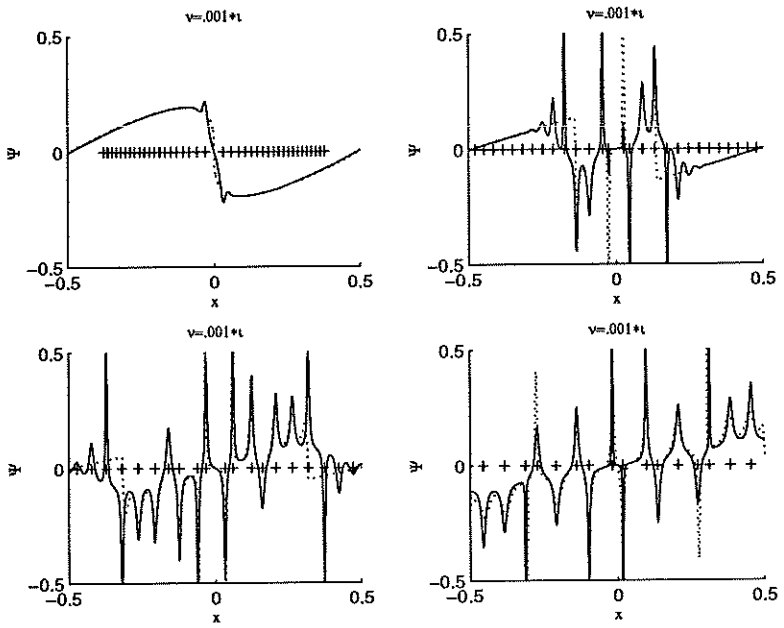

FIG. B.14. $\Re\psi_\nu(x,t)$ *vs.* x. *Comparison of pole dynamics (solid) and stationary phase approximation (dots) for* $\nu = 10^{-3} \times i$ *and* $N = 10^5$. *Projection of pole locations on the real axis (+) at* $t = 1, 2, 3, 4$.

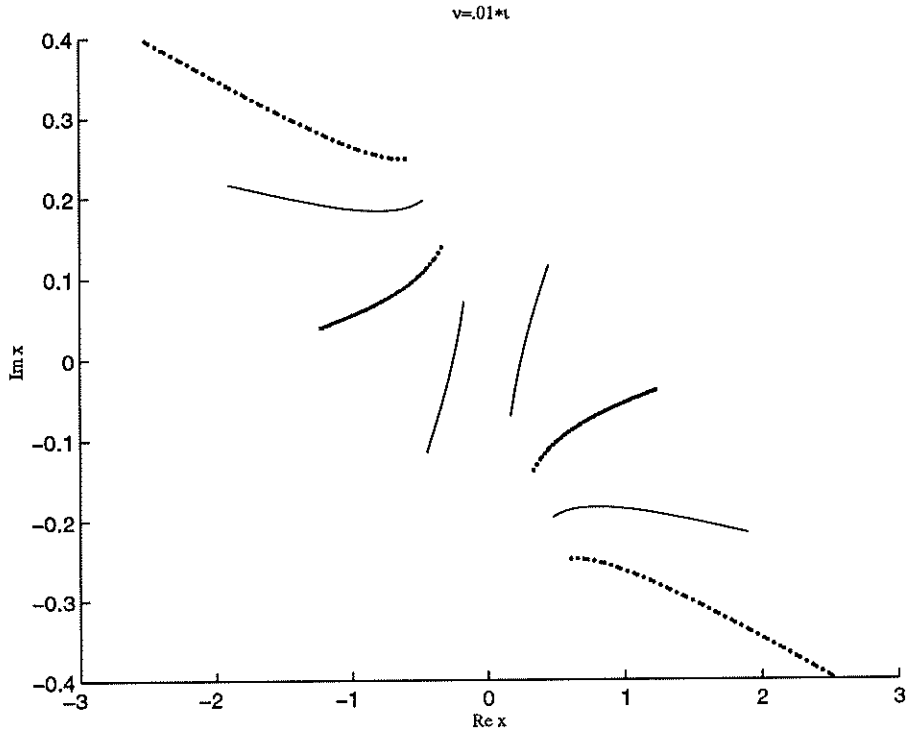

FIG. B.15. $\Im a_j(t,\nu)$ *vs.* $\Re a_j(t,\nu)$. *Time evolution in* $\mathbb{C}$ *of* $a_j(t,\nu)$, $j = -4, \cdots, 4$ *for* $\nu = 10^{-2} \times i$ *and* $N = 10^5$. $t_{initial} = t_* = 1$ *and* $t_{final} = 5$. $n_{steps} = 48$. *Typical timestep* $\delta t = .1$. *Time stepping tolerance:* $10^{-8} < L.R.T < 10^{-4}$.

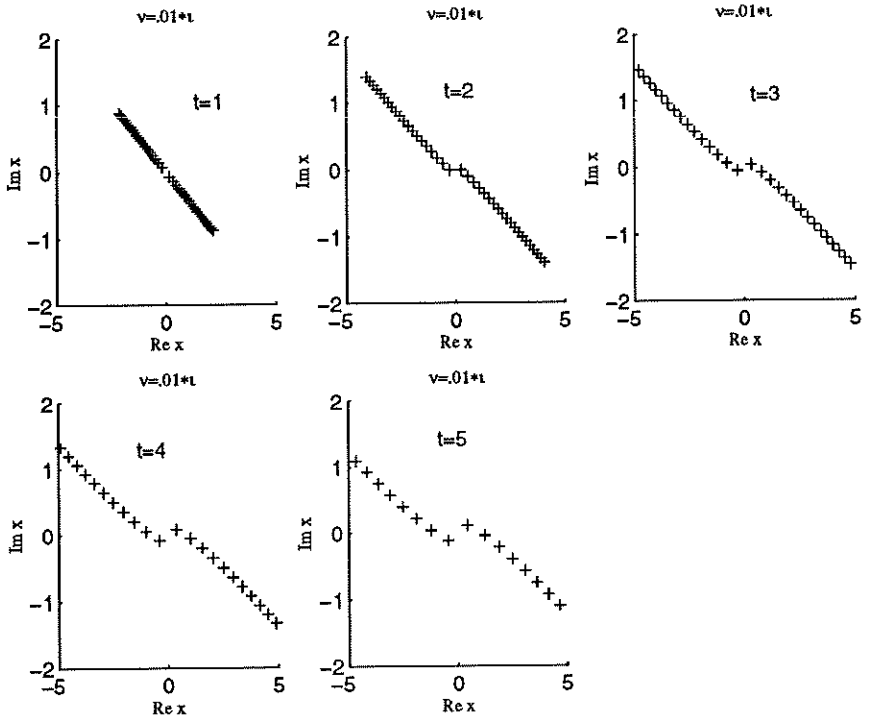

FIG. B.16. *Positions of the first 20 poles from the pole dynamics for* $\nu = 10^{-2} \times i$ *and* $N = 10^5$ *at* $t = 1, 2, 3, 4, 5$.

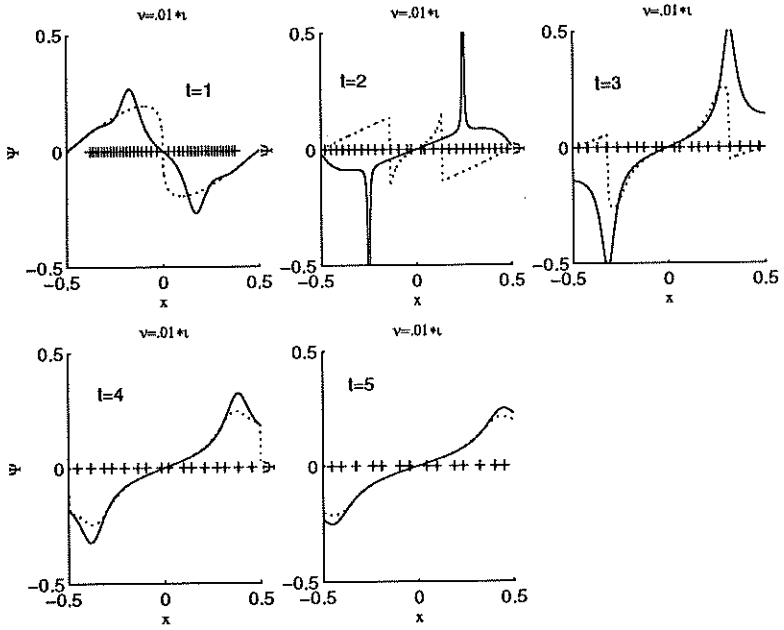

FIG. B.17. $\Re psi_\nu(x,t)$ *vs.* x. *Comparison of pole dynamics (solid) and stationary phase approximation (dots) for* $\nu = 10^{-2} \times i$ *and* $N = 10^5$ *at* $t = 1, 2, 3, 4, 5$. *Projection of pole locations on the real axis (+).*

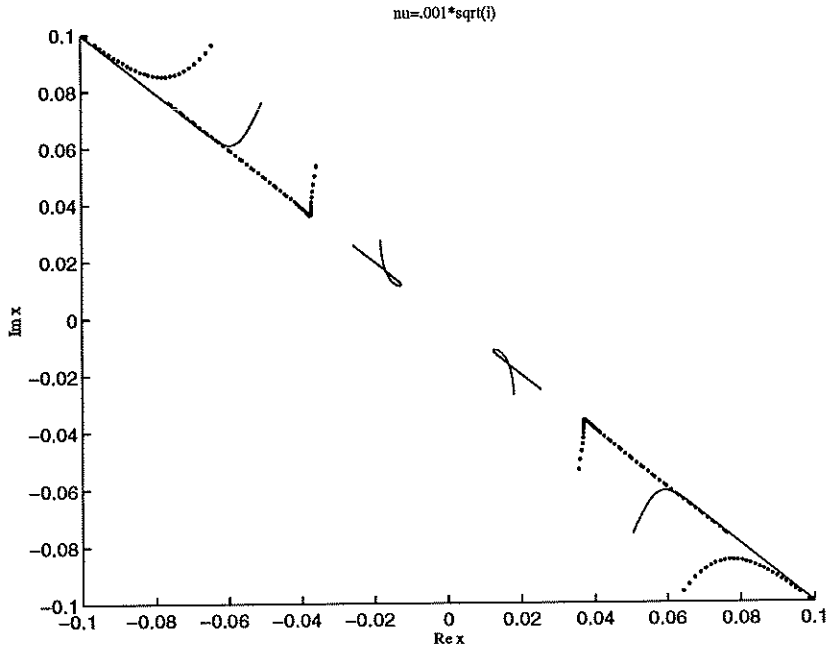

FIG. B.18. $\Im a_j(t,\nu)$ *vs.* $\Re a_j(t,\nu)$. *Time evolution in* $\mathbb{C}$ *of* $a_j(t,\nu)$, $j = -4,\cdots,4$ *for* $\nu = 10^{-3} \times e^{i\pi/4}$ *and* $N = 10^5$. $t_{initial} = t_* = 1$ *and* $t_{final} = 4$. $n_{steps} = 80$. *Time stepping tolerance:* $10^{-8} < L.R.T < 10^{-4}$.

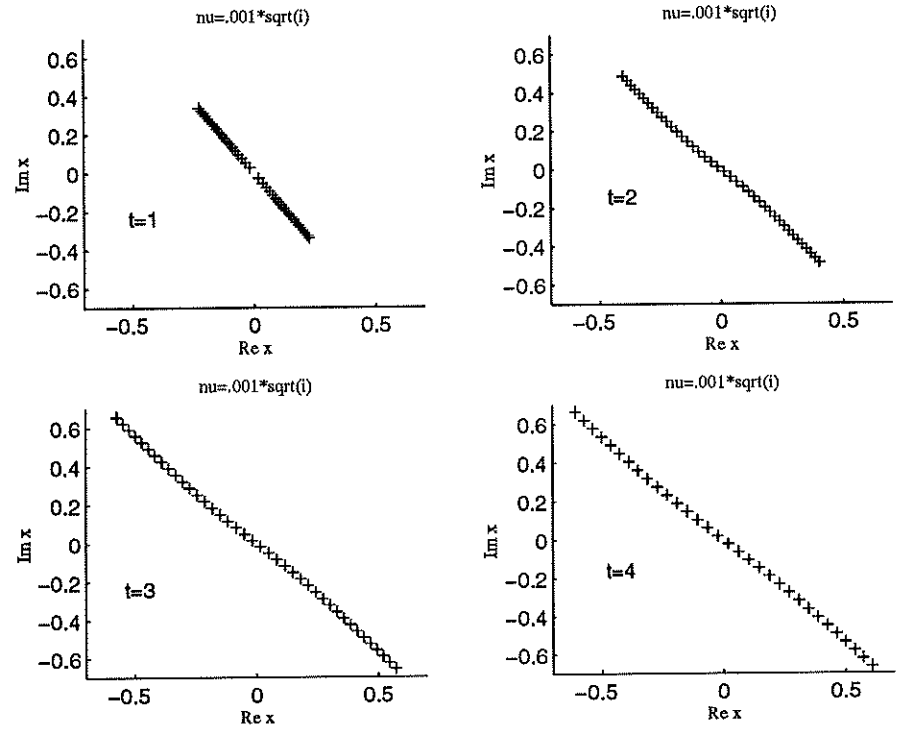

FIG. B.19. *Positions of the first 20 poles from the pole dynamics for* $\nu = 10^{-3} \times e^{i\pi/4}$ *and* $N = 10^5$ *at* $t = 1, 2, 3, 4$.

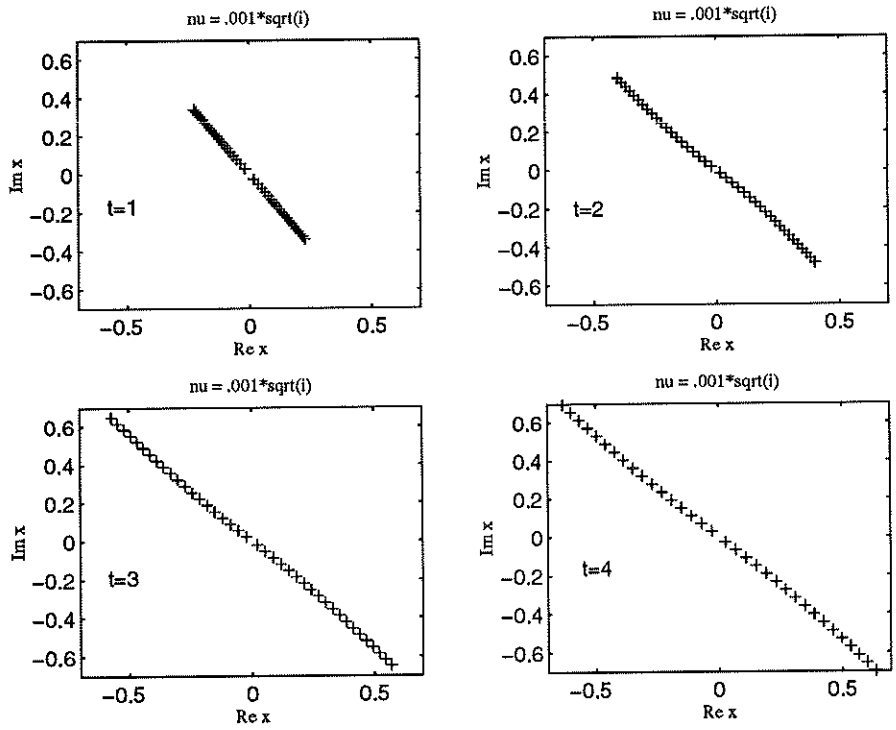

FIG. B.20. *Branch cut dynamics for* $\nu = 10^{-3} \times e^{i\pi/4}$ *at* $t = 1, 2, 3, 4$.

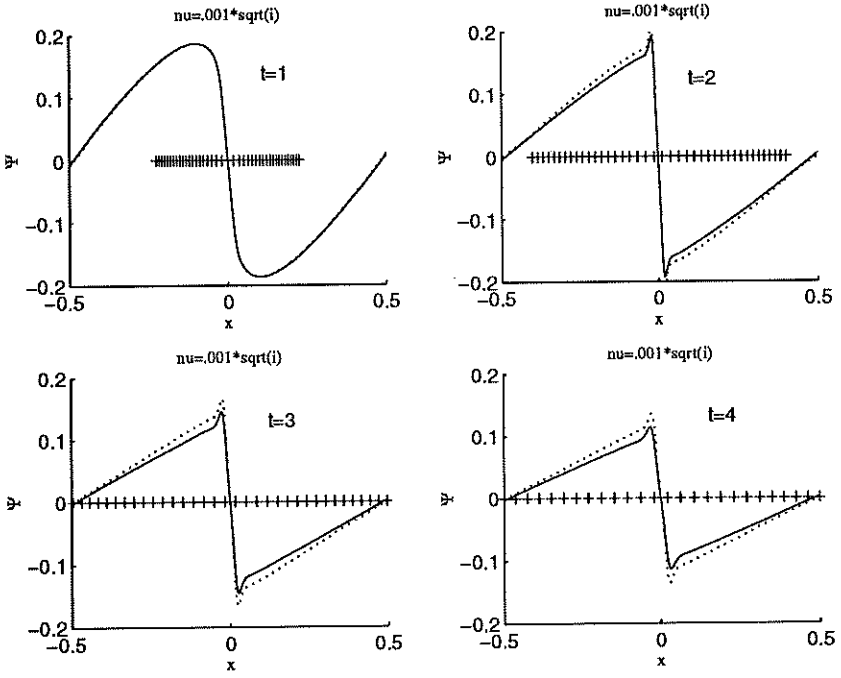

FIG. B.21. $\Re\psi_\nu(x,t)$ *vs.* x. *Comparison of pole dynamics (solid) and finite difference approximation (dots) for* $\nu = 10^{-3} \times e^{i\pi/4}$ *and* $N = 10^5$ *at* $t = 1, 2, 3, 4$. *Projection of pole locations on the real axis (+).*